



<https://technobius.kz/>

e-ISSN
2789-7338

Technobius

A peer-reviewed open-access journal

Technobius, LLP

Volume 2, No. 1, 2022



Technobius

Volume 2, No. 1, 2022



A peer-reviewed open-access journal registered by the Ministry of Information and Social Development of the Republic of Kazakhstan, Certificate № KZ00VPY00039799 dated 7.09.2021

ISSN (Online): 2789-7338

Thematic Directions: Construction and Materials Science

Publisher: Technobius, LLP

Address: 17A Momyshuly street, office 22, 010000, Nur-Sultan, Republic of Kazakhstan

Editor-in-Chief:

   *Yelbek Utepov*, PhD, Professor, Department of Civil Engineering, L.N. Gumilyov Eurasian National University, Astana, Kazakhstan

Technical Editor:

   *Assel Tulebekova*, PhD, Associate Professor, Department of Civil Engineering, L.N. Gumilyov Eurasian National University, Astana, Kazakhstan

Editors:

   *Yuri Pukhareenko*, Doctor of Technical Sciences, Professor, Department of Building Materials Technology and Metrology, Saint Petersburg State University of Architecture and Civil Engineering, Saint Petersburg, Russian Federation

   *Askar Zhussupbekov*, Doctor of Technical Sciences, Professor, Department of Civil Engineering, L.N. Gumilyov Eurasian National University, Astana, Kazakhstan

   *Evgeniya Tkach*, Doctor of Technical Sciences, Professor, Department of Building Materials Science, Moscow State University of Civil Engineering, Moscow, Russian Federation

   *Ignacio Menéndez Pidal de Navascués*, Doctor of Technical Sciences, Professor, Department of Civil Engineering, Technical University of Madrid, Madrid, Spain

   *Irina Aubakirova*, Candidate of Technical Sciences, Associate Professor, Department of Building Materials Technology and Metrology, Saint Petersburg State University of Architecture and Civil Engineering, Saint Petersburg, Russian Federation

   *Zeljko Kos*, PhD, Assistant Professor, Department of Civil Engineering, University North, Varaždin, Croatia

   *Aleksej Aniskin*, Candidate of Technical Sciences, Assistant Professor, Department of Civil Engineering, University North, Varaždin, Croatia

   *Daniyar Akhmetov*, Doctor of Technical Sciences, Associate Professor, Department of Construction and Building materials, Satbayev University, Almaty, Kazakhstan

   *Zhanbolat Shakhmov*, PhD, Associate Professor, Department of Civil Engineering, L.N. Gumilyov Eurasian National University, Astana, Kazakhstan

Copyright: © Technobius, LLP

Contacts: Website: <https://technobius.kz/>
E-mail: technobius.research@gmail.com

CONTENTS

Title and Authors	Category	No.
Nonlinear calculation of beam reinforcement using the finite element method <i>Zhanbolat Shakhmov, Shamil Amir</i>	<i>Construction</i>	0011
Features of the production of cement asphalt concrete using fuel ash <i>Kapar Aryngazin, Mariya Zhulasheva, Assem Abisheva, Aygerim Takirova, Dina Aligozhina</i>	<i>Materials Science</i>	0012
Practical experience with modified bitumen and bituminous binders <i>Zhanar Kusbergenova, Aizhan Zhankina, Timoth Mkilima</i>	<i>Materials Science</i>	0013
Refined mechanical and mathematical model of an elastic half-plane <i>Sungat Akhazhanov, Daniyar Baltabai, Bayan Nurlanova</i>	<i>Construction</i>	0014
Analysis of methods for assessing the condition of surveyed facilities in Taraz City <i>Alizhan Kazkeyev, Aleksej Aniskin</i>	<i>Construction</i>	0015



Nonlinear calculation of beam reinforcement using the finite element method

 Zhanbolat Shakhmov,  Shamil Amir*

Department of Civil Engineering, L.N. Gumilyov Eurasian National University, Nur-Sultan, Kazakhstan

*Correspondence: amir.shzh@gmail.com

Abstract. The article is devoted to the research of solution of the actual problem in construction, namely increase of ultimate loads of different kinds of constructions and possibility of effective application of innovative methods of reconstruction of beam constructions. In this work 2 kinds of different composite materials have been applied. The project considers the use of carbon fiber as an external reinforcement material for bridge girders. This study analyzes the performance of the reinforced structure under external loads. With the use of computer modeling of the finite element method, an analysis of the selection of reinforcement schemes, which allows to significantly increase the carrying capacity of reinforced concrete beam structures, is performed. Also, some proposals for the implementation of these experiments on real girder structures and constructions were considered. The data obtained as a result of the work allow the conclusion about the successful application of composite materials as reinforcement structures. Correctly chosen scheme of strengthening, confirmed by calculations allows you to significantly increase the carrying capacity of the beam reinforced concrete structures.

Keywords: beam reinforced concrete structures, composite materials, finite element, elastic modulus, the law of nonlinear deformation, mosaic of stresses, stress diagram.

1. Introduction

Currently, due to the growth of population in large cities, the construction of pedestrian and vehicular bridges is justified because of the increase in general traffic and increased traffic jams. But with the high cost of new construction, it is important to make reconstruction of old structures. In near future we will have to reconstruct actively the old highways to be able to pass traffic flows with high intensity, which will increase the load on the artificial structures of the road network. In addition, there is a constant tightening of standards and normative loads at which new bridges should be designed and existing bridges should be reconstructed. Changes in construction standards and increased loads lead to the need reinforcing bridge spans, increasing their bearing capacity. In addition, various defects and damages associated with both external adverse environment and physical deterioration of the structure constantly arise in the bridge structures during operation.

Composite materials based on carbon fibers have the following advantages:

1. The tensile strength is much higher than the reinforcing steel used;
2. Composite materials are easy to prestress;
3. The material can be used for reinforcement of reinforced concrete structures of any type, as due to its plasticity it repeats their design;
4. Composite materials can be used to reinforce structures with any radius of curvature;
5. It is allowed to install the composite material without stopping the exploitation of the construction;
6. The small thickness of the strips of composite material (from 1.5 to 2.0 mm) allows you to install them simultaneously in two directions to increase the carrying capacity of the structure.

B27.5	2.5	$3 \cdot 10^6$	0.2	1458.6 (14.3)	2106.867 (20.656)	107.1 (1.05)	178.5 (1.75)
-------	-----	----------------	-----	------------------	----------------------	-----------------	-----------------

Table 2 – Accepted reinforcement characteristics

Name	Sectional diameter, d, cm	Sectional area, A, cm ²	Modulus of elasticity, E _s , t/m ² (MPa)	Calculation resistance of the reinforcement to tension, R _s , t/m ² (MPa)	Standard tensile strength of the reinforcement, R _{sn} , t/m ² (MPa)
Working rebar:					
Ø28AIII (A400)	2.8	6.1544	$204 \cdot 10^5$	35700	40209
Ø16AIII (A400)	1.6	2.0096	$(2,0 \cdot 10^5)$	(350)	(394.211)
Clamps:					
Ø8AI (A240)	0.8	0.5024	$214.2 \cdot 10^5$	21420	33821
2xØ8AI (A240)	1.13	1.0048	$(2.1 \cdot 10^5)$	(210)	(232.105)

2.3 Manual calculation

Calculation of bendable reinforced concrete elements is made according to SP 35.13330.2011 Bridges and pipes. The scheme of forces and the stress diagram in the cross-section normal to the longitudinal axis of an eccentrically compressed concrete element is shown in the following Figure 2 [6].

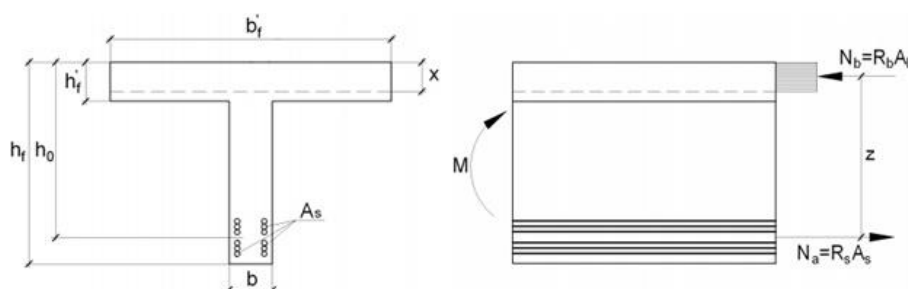


Figure 2 – Geometric section of a T-beam and stress diagram in the section

As a result of manual calculation, we obtain the following values:

The height of the compressed zone of concrete - 12.34 cm
 The maximum allowable value of bending moment - 205.86 t/m
 Conditional uniformly distributed load q, under the action of which in the beam the resulting moment occurs - 5.496 t/m (or 4.185 t/m² for uniformly distributed over the area of the beam plate load) [7].

2.4 Calculation in SP LIRA-SAPR

The basis of the method of calculation of reinforced concrete structures for bending is based on experimental data accumulated over many years of laboratory research. These data testify to the fact that as the bending moment M increases, the reinforced concrete element under consideration passes through three fundamentally different stages of the stress-strain state [8]. The first stage is characterized by the absence of cracks in the tensile part of the concrete. This corresponds to the level of effective tensile stresses below the ultimate strength R_{bt}. The second stage is characterized by the formation of cracks in the tensile zone of the concrete due to the exceeding of the acting stresses of the value R_{bt}. The formation of cracks leads to redistribution of stresses in the cross-section, the concrete in the tensile zone is gradually disconnected from the work. The moment of appearance of noticeable plastic deformations of the reinforcement is, in its turn, the beginning of the third stage of failure.

Therefore, it is necessary to take into account the physical non-linearity of deformation of reinforced concrete beams shown in the Figure 3 [9-10].

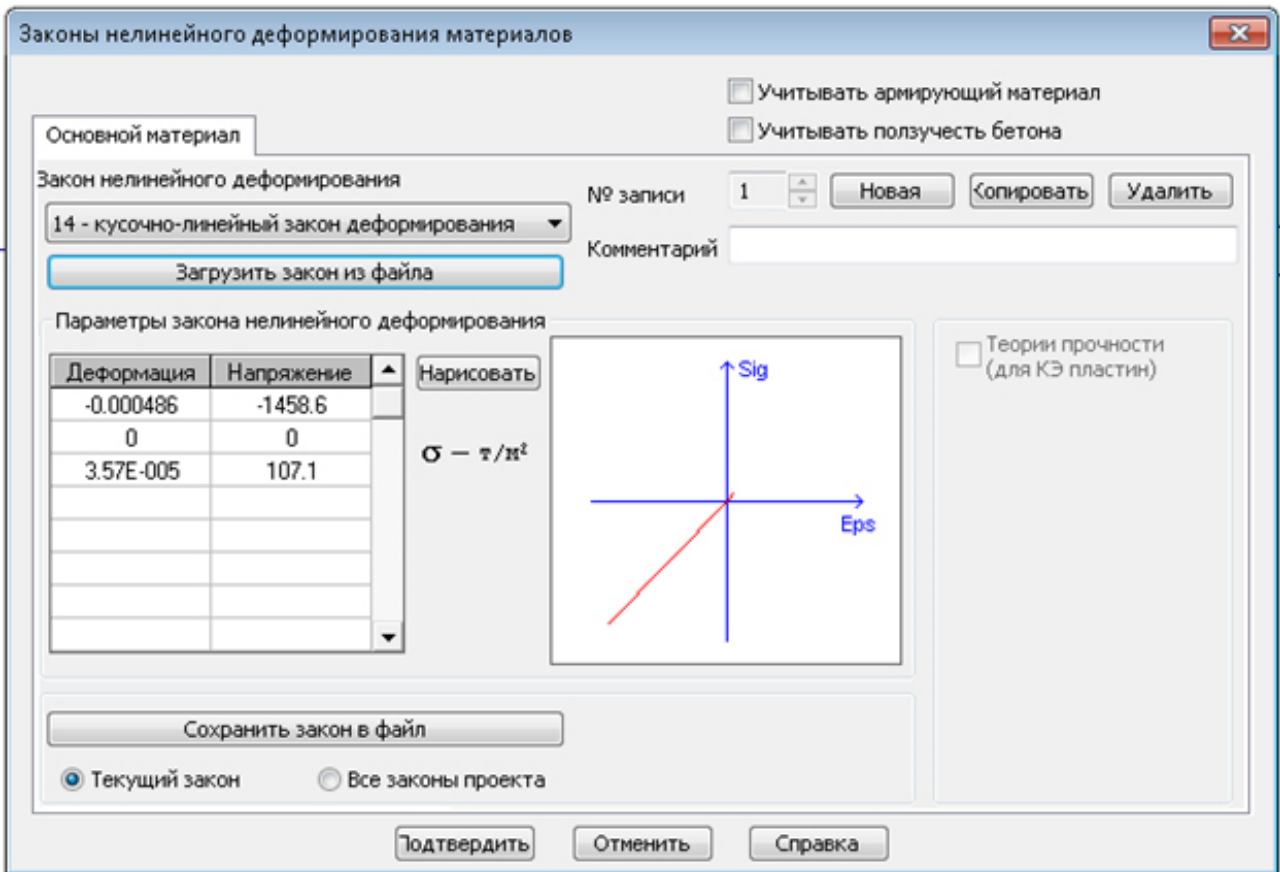


Figure 3 – Consideration of the law of nonlinear deformation of materials in SP LIRA-SAPR

During the calculation, you can immediately observe how the concrete collapses in the tensile zone in the Figure 4.

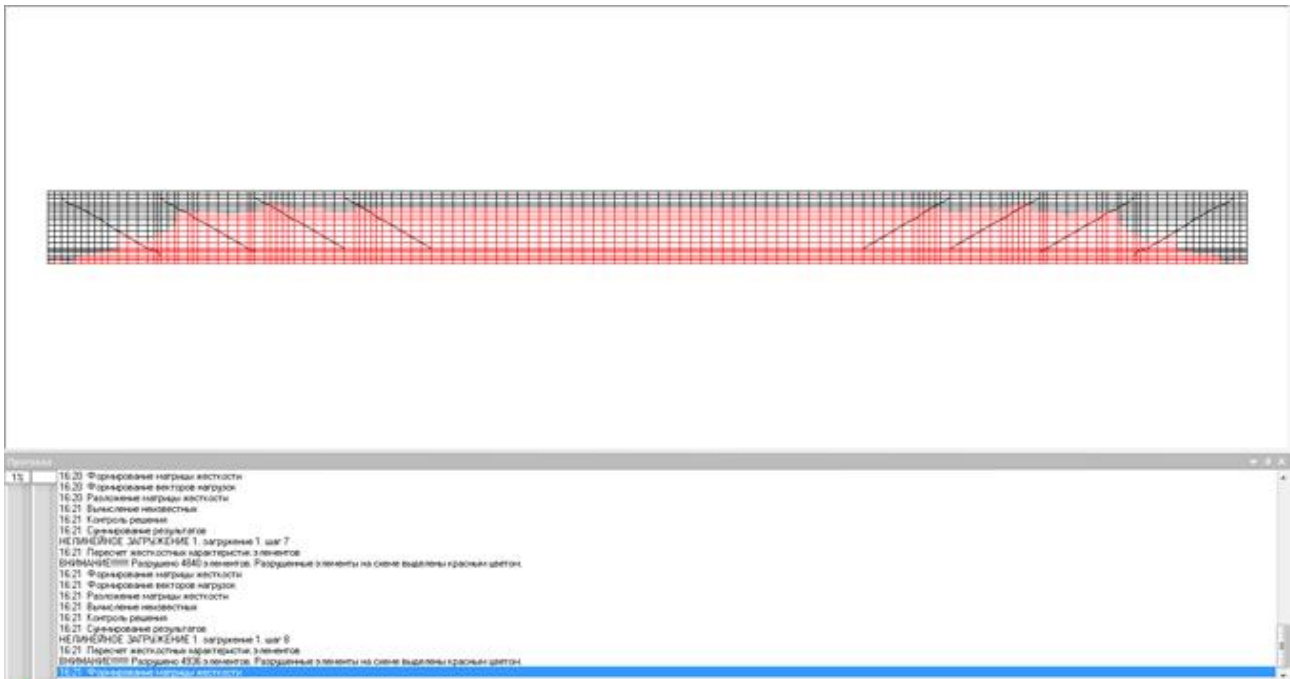


Figure 4 – Calculation process in the program

The mosaic of stresses in the middle of the beam span from the action of conditional uniformly distributed load corresponding to M_{ult} demonstrated in the Figure 5 [11]. The greatest stresses in the

working reinforcement: 35625 t/m^2 , which almost corresponds to the design tensile strength of the reinforcement $R_s=35700 \text{ t/m}^2$.

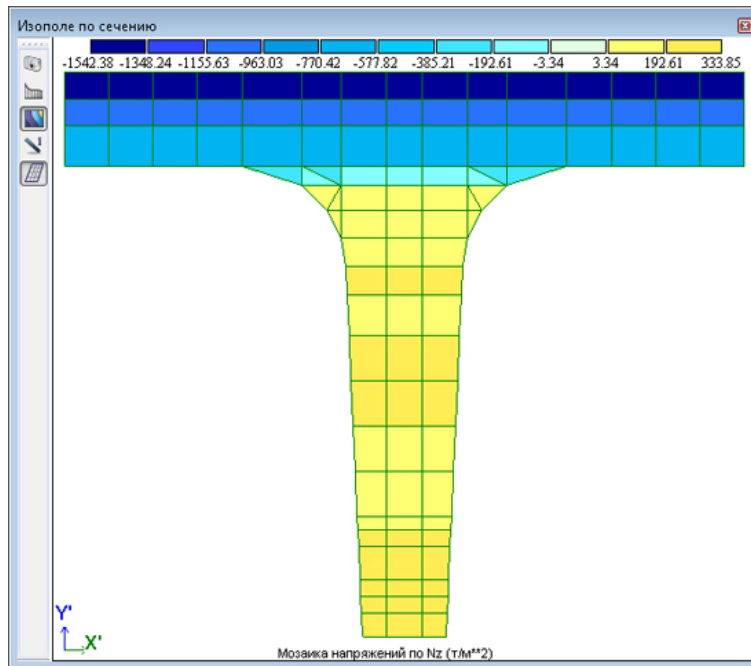


Figure 5 – Stresses in the concrete compression zone

As can be seen, the stresses in the compressed zone of the concrete exceeded the value of the design resistance of concrete to compression. This can be explained as follows. In our calculation, the linear law of deformation was taken, so the stress diagram of the compressed zone of concrete has a triangular form (Figure 6a). In the calculation of destructive forces (manual), the stress diagram has a rectangular outline (Figure 6b) [12-13]. Therefore, we shall take the value of 1542.38 t/m^2 as a destructive stress acting in the compressed zone. In the future, when calculating the reinforced models of the beam, we will rely on this value as the maximum permissible one.

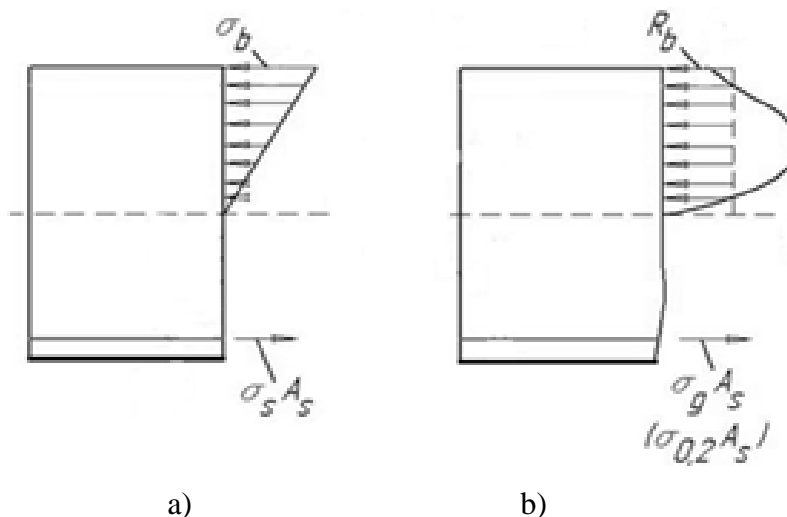


Figure 6 – Stress diagram of the compressed zone

2.5 Beam reinforcement with composite materials

Strengthening with MBRACE LAM CF210/2400.120x1.4.100m lamellas (at the bottom of the beam) - scheme 1. Strengthening with MBRACE LAM CF210/2400.120x1.4.100m slats (along the side edges of the beam ribs) - scheme 2. Strengthening with FibARM Tape - 230/300 - scheme 3 (Figure 7).



Figure 7 – Beam strengthening with composite materials: a – according to scheme 1; b – according to scheme 2; c – according to scheme 3

The following grades of composite materials were used for strengthening shown in the Table 3.

Table 3 – Characteristics of composite materials

Name	Modulus of elasticity, E_f , t/m^2 (MPa)	Tensile strength, R_f , t/m^2 (MPa)	Thickness, mm	Width, mm
MBRACE LAM	$2,142e^7$	$244,8e^3$	1.4	120
CF210/2400.120x1.4.100m (LAMEL)	(210 000)	(2400)		
FibARM Tape – 230/300 (unidirectional carbon tape)	$2.346e^7$ (230 000)	$438.6e^3$ (4300)	0.128	300

3. Results and Discussion

Mosaic of stresses in the middle of the beam span from the action of the load causing maximum allowable stresses in the compressed zone of concrete. Strengthening with MBRACE LAM CF210/2400.120x1.4.100m (at the bottom of the beam rib) (Figure 8).

Maximum stresses in the working reinforcement: $35652 t/m^2 < R_s=35700 t/m^2$.

Maximum stresses in lamella: $40072 t/m^2 < 244800 t/m^2$.

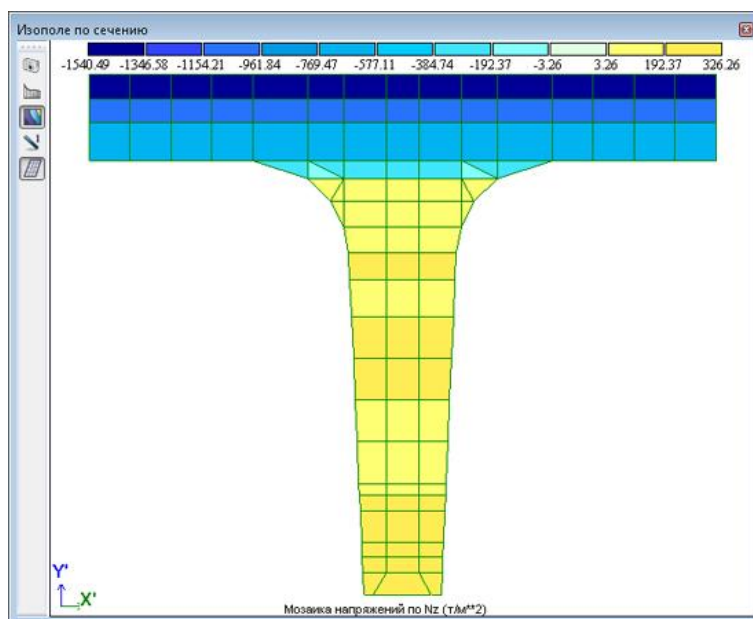


Figure 8 – Mosaic of stresses in the middle of the beam strengthened according to scheme 1

Mosaic of stresses in the middle of the beam span from the action of the load causing maximum allowable stresses in the compressed zone of concrete. Strengthening with MBRACE LAM CF210/2400.120x1.4.100m (along the side edges of the beam ribs) (Figure 9).

Maximum stresses in the working reinforcement: $35415 \text{ t/m}^2 < R_s=35700 \text{ t/m}^2$.

Maximum stresses in lamella: $98565 \text{ t/m}^2 < 244800 \text{ t/m}^2$.

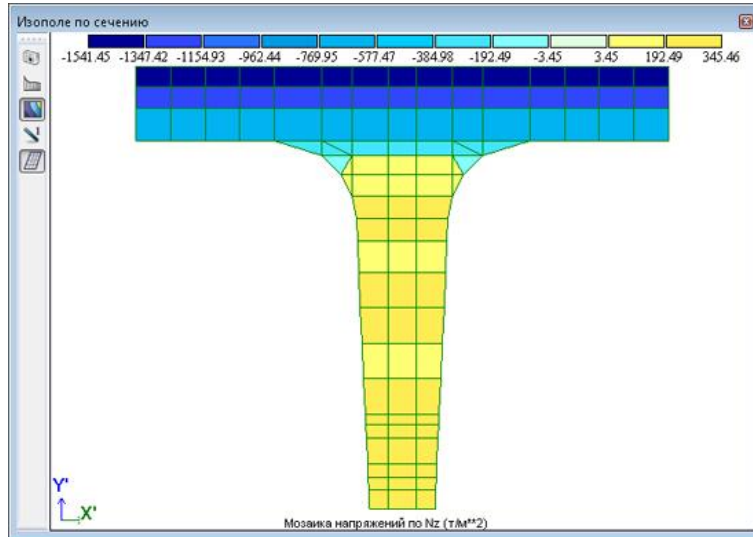


Figure 9 – Mosaic of stresses in the middle of the beam strengthened according to scheme 2

Mosaic of stresses in the middle of the beam span from the action of the load causing maximum allowable stresses in the compressed zone of concrete. Strengthening with FibARM Tape - 230/300 (Figure 10).

Maximum stresses in the working reinforcement: $35455 \text{ t/m}^2 < R_s=35700 \text{ t/m}^2$.

Maximum stresses in lamella: $42456 \text{ t/m}^2 < 438600 \text{ t/m}^2$.

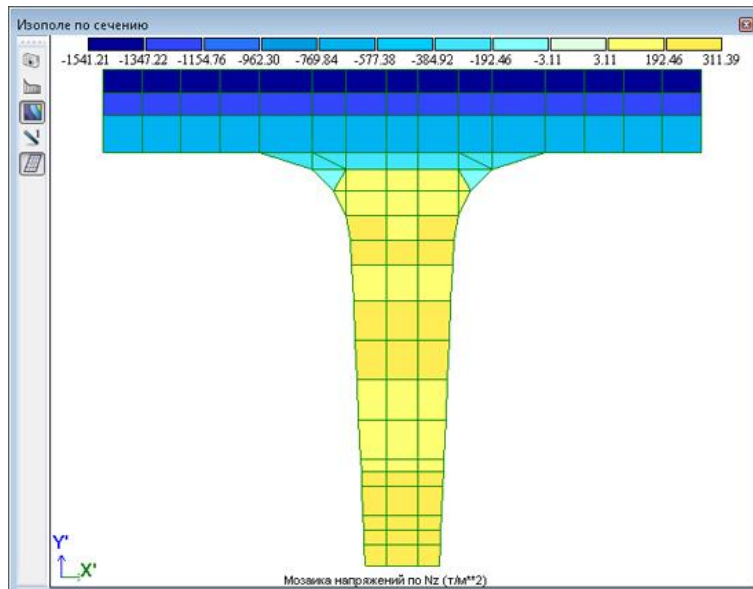


Figure 10 – Mosaic of stresses in the middle of the beam strengthened according to scheme 3

Table 4 below shows the comparative analysis of the results of strengthening.

Table 4 – Comparative analysis of the results of strengthening

Calculation	Load value (t/m^2)	Increment of the maximum allowable load [%]
-------------	----------------------------------	--

Regular beam	4.185	0
Strengthening according to scheme 1	4.28	2.3
Strengthening according to scheme 2	4.43	5.9
Strengthening according to scheme 3	4.37	4.4

According to this table, it can be argued that when using composite material to strengthen the beam structure, the maximum permissible load increased in the 1st scheme by 2.3%, in the 2nd scheme by 5.9% and, respectively, in the 3rd scheme by 4.4%. Thus, the maximum increase of 5.9% is observed in the 2nd scheme.

In the article of V.L. Chernyavskiy, P.P. Osmak "Strengthening of Reinforced Concrete and Brick Structures Using Composite Materials" the positive results of application of composite material in the strengthening of beam reinforced concrete, slab reinforced concrete and brick structures are reported. In particular, the data given in the above article are not confirmed by specific calculations and laboratory studies. In general, taking into account the correctness of the approach (direction) of the solution of this particular situation, in my work was extended general scientific approach to the problem in question using various calculations and 3D modeling.

4. Conclusions

The following research objectives were achieved in this paper:

1. The design of reinforced concrete T-beam reinforced with composite material in PC LIRA-SAPR has been simulated.
2. A comparative analysis between different reinforcement schemes has been carried out.
3. The change in the maximum allowable load acting on the beam after the reinforcement has been traced.

The data obtained as a result of the work allow drawing a conclusion about the successful application of composite materials as reinforcement structures. Correctly chosen scheme of reinforcement, confirmed by calculations allows significantly increase the bearing capacity of girder reinforced concrete structures. These conclusions can be recommended for application of the considered composite materials, taking into account increase of limiting loads on structures in various sectors of construction.

References

1. Probabilistic models of reliability of information and computing systems / Ushakov I.A. — Moscow: Radio and Communication, 1991. — P. 82-89.
2. Finite element method, SP LIRA-SAPR / LiraLand group of companies // LiraLand. — [2018]. — Access mode: <https://www.liraland.ru/solutions/functionality/fem.php>
3. FEM processors, SP LIRA-SAPR [Electronic resource] / LiraLand group of companies // LiraLand. — [2016]. — Access mode: <https://www.liraland.ru/lira/systems/processor.php>
4. Reliability Theory / V.A. Ostreykovskiy. — M. Higher school, 2003. — P. 102-109.
5. GOST 27751-2014 Electrical articles. Reliability and safety of building structures and foundations. Basic provisions. — 2014.
6. SP 35.13330.2011 Electrical articles. Bridges and pipes. Updated version of SNiP 2.05.03-84*. — 2011.
7. Library database / SP Lira-SAPR. — LiraLand, 2021
8. Fundamentals of the theory of reliability / A.M. Polovko, S.V. Gurov — St. Petersburg: publishing house BHV-Petersburg, 2008. — P. 177-184.
9. Nonlinear analysis of whole deformation process of RC T-beam strengthened with carbon fibers / World Earthquake Engineering // Heilongjiang Institute of Technology — [2018]. — Access mode: https://en.cnki.com.cn/Article_en/CJFDTotal-SJDC201004028.htm
10. Nonlinear behavior analysis of flexural strengthening of RC beams with NSM FRP laminates / Y. Yang, M.F.M. Fahmy, J. Cui, Z. Pan, J. Shi // Structures. — 2019. — Vol. 20. — P. 374 – 384. <https://doi.org/10.1016/j.istruc.2019.05.001>
11. Capacity assessment of older t-beam bridges by nonlinear proxy finite-element analysis / A.P. Schanck, W.G. Davids // Structures. — 2020. — Vol. 23. — P. 267–278. <https://doi.org/10.1016/j.istruc.2019.09.012>

12. Design features of bimetallic bridges / A. Makarov, S. Kalinovsky // E3S Web of Conferences. — 2019. — Vol. 97. No. 06001. <https://doi.org/10.1051/e3sconf/20199706001>
13. Linear and nonlinear model updating of reinforced concrete T-beam bridges using artificial neural networks / O. Hasançebi, T. Dumlupınar // Computers & Structures. — 2013. — Vol. 119. — P. 1-11. <https://doi.org/10.1016/j.compstruc.2012.12.017>

Information about authors:

Zhanbolat Shakhmov – PhD, Associated Professor, Department of Civil Engineering, L.N. Gumilyov Eurasian National University, Nur-Sultan, Kazakhstan, zhanbolat8624@mail.ru

Shamil Amir – Master Student, Department of Civil Engineering, L.N. Gumilyov Eurasian National University, Nur-Sultan, Kazakhstan, amir.shzh@gmail.com

Author Contributions:

Zhanbolat Shakhmov – concept, methodology, resources, analysis, funding acquisition, editing.

Shamil Amir – data collection, testing, modeling, interpretation, visualization, drafting.

Received: 06.02.2022

Revised: 14.02.2022

Accepted: 14.02.2022

Published: 10.03.2022



Features of the production of cement asphalt concrete using fuel ash

Kapar Aryngazin¹, Mariya Zhulasheva^{*1}, Assem Abisheva², Aygerim Takirova³,
 Dina Aligozhina⁴

¹Department of Architecture and Design, Toraighyrov University, Pavlodar, Kazakhstan

²Department of Civil Engineering, L.N. Gumilyov Eurasian National University, Nur-Sultan, Kazakhstan

³Department of Chemistry, Chemical Technology and Ecology, Kazakh University of Engineering and Technology, Nur-Sultan, Kazakhstan

⁴Department of Biology and Ecology, Toraighyrov University, Pavlodar, Kazakhstan

*Correspondence: mariya_98.kz@mail.ru

Abstract. In this work, the objects of research are cement asphalt concrete obtained on the basis of cement binder and bitumen emulsion, using as mineral additives, waste from thermal power plants, in the form of fuel ash of various types. The analysis of foreign and domestic literature on this topic is carried out. In order to reduce the amount of inorganic binder (cement) consumed, as well as modification of organic binder (bitumen emulsion), fuel ashes of two domestic producers, ashes of CHP-2 and CHP-3 of Pavlodar based on Ekibastuz coals, were studied in the work. The influence of fuel ash on the properties of binders used in the work, as well as the properties of cement asphalt concrete compositions based on binders using fuel ash, has been established. The features of the production of cement asphalt concrete using fuel ash are described. The results of testing cement asphalt concrete without the use and with the use of fuel ash are presented.

Keywords: cement asphalt, plants, ash, waste, industry, building materials.

1. Introduction

The Republic of Kazakhstan speaks of the need to develop a environmentally friendly economy and closed production cycles, which implies "constant management of the material cycle in production and consumption, excluding the formation of waste that accumulates in the environment." It still contains a huge amount of ash and slag. Waste from thermal power plants and metallurgical waste at old landfills, which, unfortunately, continue to accumulate every year, which requires the development of new initiatives to implicate them in recycling [1].

Due to the high cost of road construction materials, the issues of using new technologies, efficient and unconventional materials, waste and by-products of industry in road construction are of particular importance. First of all, this applies to such technologies and materials that could improve the quality of asphalt concrete coatings, reduce the consumption of expensive binders of petroleum origin. The technologies under consideration also provide opportunities for the use of high-tonnage waste and industrial by-products as part of asphalt concrete mixtures.

The issues of the use of high-tonnage waste and by-products of industry are also important because they allow simultaneously solving the problem of the environmental plan - to free up vast territories of land occupied by waste, to prevent environmental pollution [2].

Studies were conducted to evaluate the ability of nanoparticles to reduce the temperature sensitivity of the mechanical properties of cement-asphalt mortar and to study the mechanism of the influence of nanoparticles on thermal characteristics. First, bending and compression tests of cement-asphalt mortar with nano-SiO₂ and nano-TiO₂ were carried out at five various temperatures varying

from -20 °C to 60 °C, and the bending and compressive strength were measured. Based on the experimental results, the type, number of nanoparticles and the effect of temperature sensitivity on flexural and compressive strength were studied. In addition, changes in the composition and microstructure of cement-asphalt mortar were studied using a scanning electron microscope, and the temperature-related behavior of cement-asphalt mortar is explained on the basis of experimental observations [3].

Asphalt-Portland cement concrete has the properties of both flexible and rigid concrete. A laboratory study was conducted to evaluate the effectiveness of asphalt-Portland cement concrete composite under controlled conditions. The program included the following tests: stability, indirect tensile strength, compressive strength, modulus of elasticity, sensitivity to water, freezing and thawing, as well as resistance to chloride penetration [4]. The tests were carried out at three levels of wet curing: no wet curing, one-day wet curing and three-day wet curing. The samples were tested for 28 days. The results were compared with the results of control samples of hot-mix asphalt concrete and Portland cement concrete. The study concluded that the strength and durability properties of asphalt-Portland cement concrete composite are better than those of asphalt with a hot mixture. It was found that the penetration of chloride into the samples is less than in ordinary Portland cement concrete. The study shows that asphalt-Portland cement concrete composite is an effective alternative material for use as a bridge flooring coating [5].

The effect of cement kiln dust as a filler on the low-temperature characteristics of hot mix asphalt concrete was investigated. A laboratory program consisting of an assessment of the durability of asphalt concrete of a hot mixture in freeze-thaw cycles using indirect tensile strength testing and analysis of fatigue behavior at four temperatures of 20, 0, -10 and -20 °C using a four-point bending fatigue test. In addition, an environmental assessment was carried out with respect to the presence of heavy metals in the dust compounds of the cement kiln by applying a leaching toxicity test. According to the results obtained, mixtures containing cement kiln dust filler demonstrated better resistance to freeze-thaw cycles compared to the control mixture containing limestone. In addition, mixtures containing cement kiln dust showed a higher fatigue life compared to the control mixture, and for all mixtures, fatigue life decreased due to a decrease in temperature [6]. However, at lower strain levels of 150 micro-stresses, the fatigue life of the studied mixtures was largely similar, and even higher fatigue life was obtained by reducing the test temperature. In addition, the results of the toxicity test by leaching showed that the number of heavy metals in the filtrate from asphalt concrete hot mixture containing cement kiln dust was low and met the required criteria [7].

The composition of cement-asphalt concrete mixture is characterized in the invention. Technical result: reduction of the amount of complex binder while improving the physical and mechanical properties of the resulting material: increased water resistance and long-term water resistance, resistance to alternate freezing and thawing, increased modulus of deformation and strength [8].

The purpose of the experimental investigations was to obtain a hollow wall stone based on ash and slag waste with a strength not inferior to products made according to a usual recipe. A study was carried out with selected samples of bauxite sludge from the sludge dumps of the Pavlodar Aluminum Plant, as fillers was used metallurgical slag of fractions 0-5 and 20-30 according to 6 recipes made in forms 100x100x100 mm. The resulting samples with various ratios of components in the mixture were examined for compressive strength, moisture absorption, and frost resistance. It has been established that when ash and slag waste is added to the concrete mixture in an amount of up to 35 % by weight of dry components, the strength characteristics of the hollow wall stone correspond to the selected brand [9].

2. Methods and Materials

Studies of raw materials, binders using mineral additives, as well as compositions of final composites were carried out using the material and scientific and technical base of the NAO "Toraigyrov University".

When evaluating the combustion products of coal in a hot asphalt-concrete mixture, it was found that the combustion products of fine coal are a by-product of coal combustion in the production of electricity. Fly ash is commonly used in Portland cement concrete. However, some fly ash was used in hot mix asphalt concrete as mineral fillers. Due to the current changes in environmental protection requirements for emissions, large volumes of fly ash containing sulfur cannot be used in traditional concrete. Therefore, this study was undertaken in order to find out whether some of the smaller evils could be usefully used in hot mix asphalt concrete. In this project, fly ash was mixed with asphalt binder PG 58 - 28 in various percentages (5 %, 10 % and 15 %). A rotational viscosity test was carried out on the mixture to determine what percentage of fly ash by weight of asphalt binder would be acceptable. All percentages were deemed viable [10].

Then Hamburg tests were carried out tracking these mixtures of asphalt concrete hot mix. The stages of sample preparation included: drying of aggregates to a constant weight, dosing of aggregates, heating of aggregates and binder to the mixing temperature, mixing of binder and aggregates, conditioning (short-term aging) and compaction of the sample to the appropriate percentage of voids using the gravity machine "Superave" compactor. The process of mixing asphalt concrete with a hot mixture is shown in Figure 1.



a)



b)



c)



d)

Figure 1 – The process of mixing asphalt concrete with a hot mixture: a) Heating aggregate to mixing temperature; b) Adding asphalt to the aggregate in the mixer; c) Mixing of asphalt and aggregate in the mixer; d) Mixture kept at compaction temperature for 2 h.

The compaction of the sample using the gravity machine "Superave" compactor is shown in Figure 2.

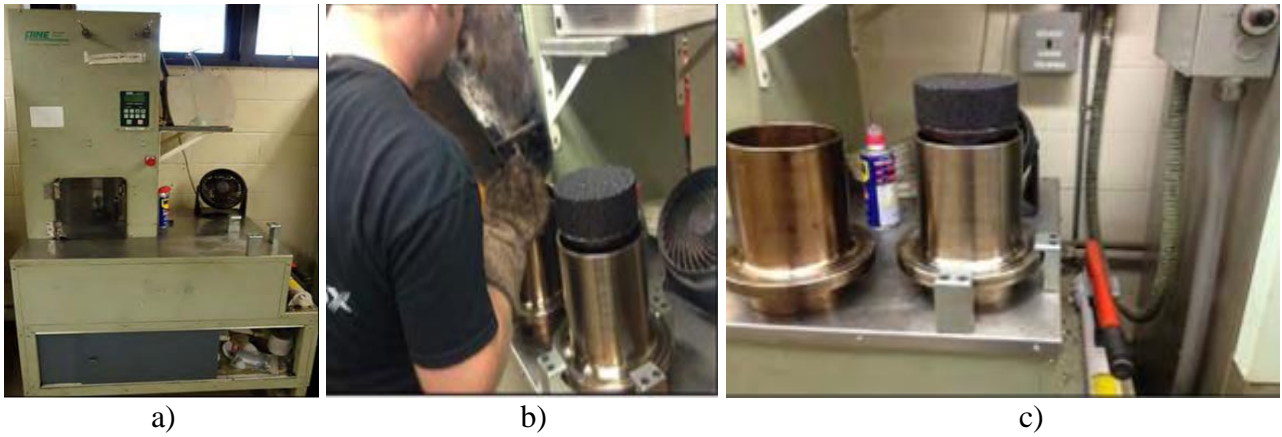


Figure 2 – Compaction of the sample using a gravity machine "Superave": a) Pine Superpave Gyrotory compactor; b) Pouring HMA into SGC mold; c) Extruding the sample from the mold

The stages of the Hamburg test are shown in Figure 3.

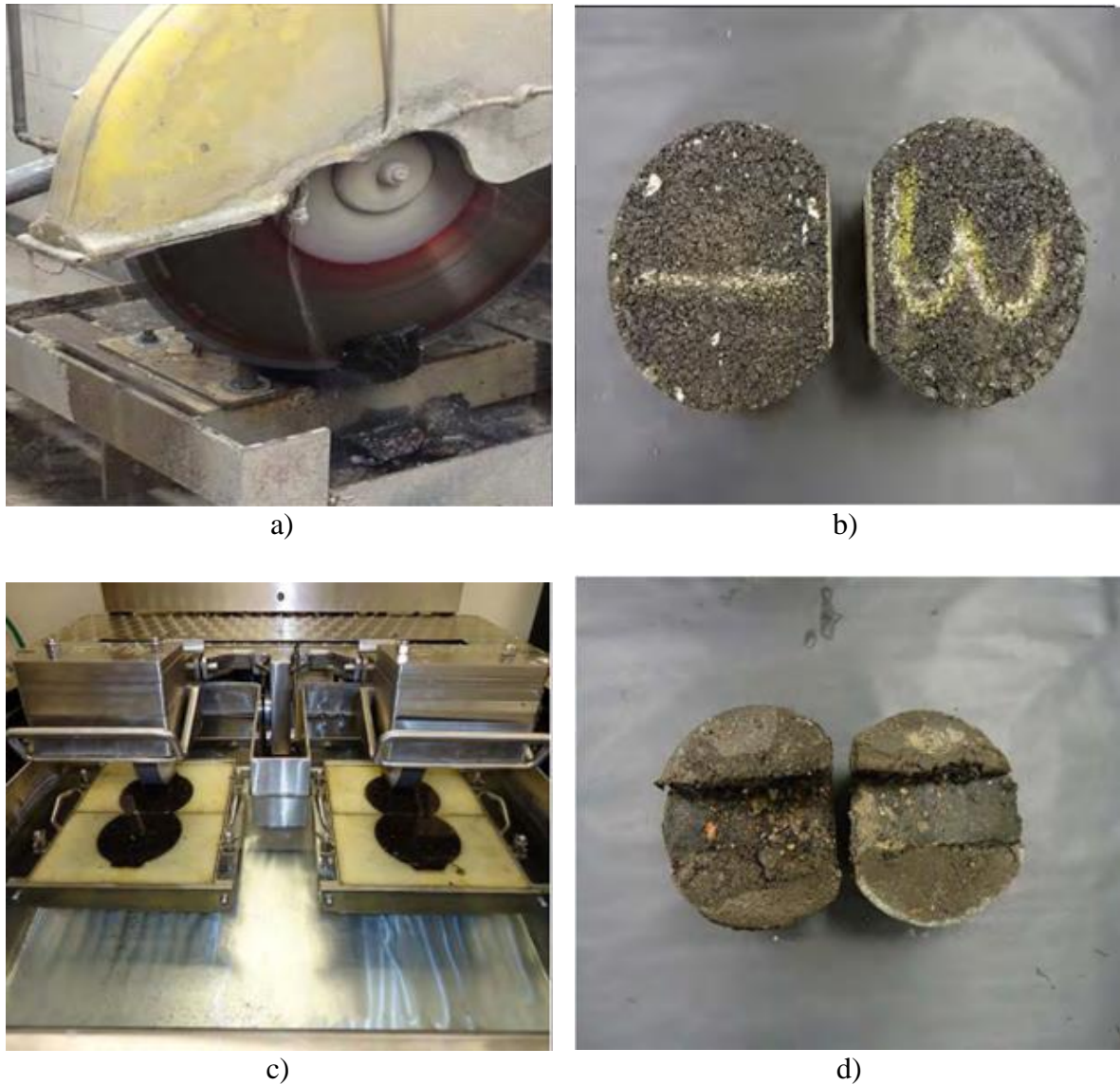


Figure 3 – Testing stages: a) Sample is cut along the edge of the mold; b) Vertical-cut sample; c) Spicements placed in molds and mounted in tray; d) Failed sample (rut depth >20 mm)

Based on the results of the Hamburg test, the most effective mixture with 15% fly ash was selected for further tests, such as modified Lottman, dynamic module and S-VECD test, and comparison with the control group (without fly ash). The results showed positive dynamics [11].

Features of the production of cement asphalt concrete using fuel ash. Taking into account the formation of an optimal structure, as well as for effective quality control of both raw materials and cooking technology, one of the most rational methods was used in the work – separate and sequential mixing. This technology consists in separate preparation of cement-ash-sand mortar with fine aggregate (sand) and black crushed stone (crushed stone treated with an emulsion using ash), after which they are supposed to be mixed together. Figure 4 shows a scheme for obtaining cement asphalt concrete.

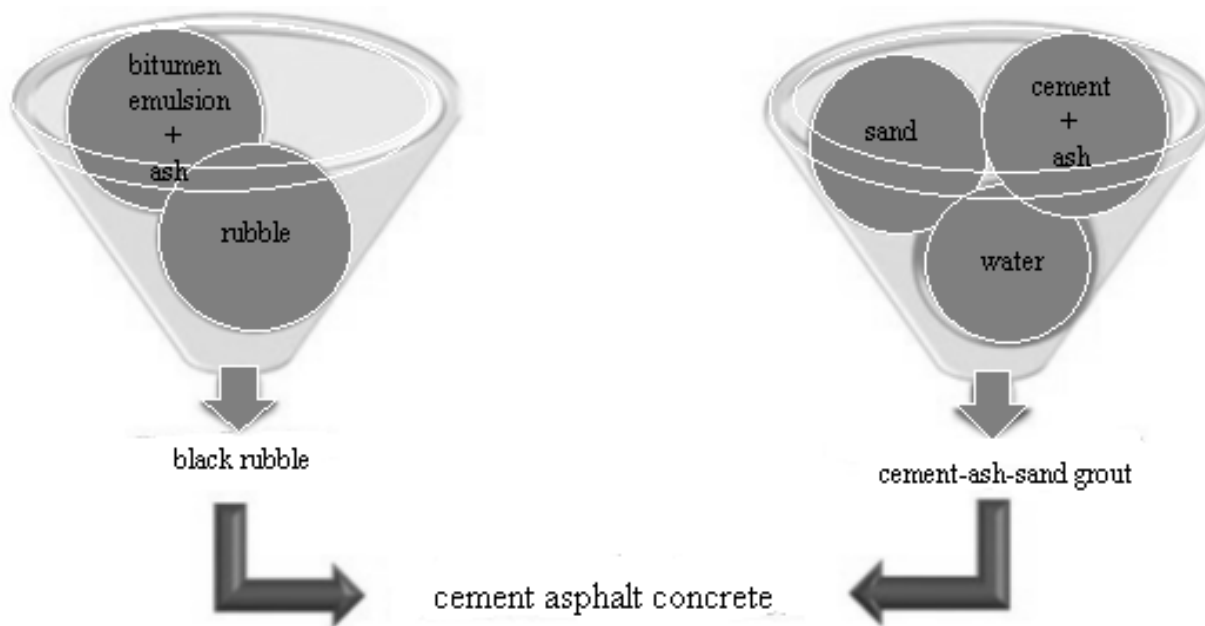


Figure 4 – Scheme for obtaining cement asphalt concrete

Separate mixing of crushed stone with bitumen emulsion, in this case modified with mineral additives in the form of fuel ash, allows you to regulate the distribution of bitumen over the surface of crushed stone (reducing the area of coating of crushed stone grains with bitumen by about a third, up to 60-70%), ensuring its contact directly with cement stone. The distribution of bitumen over the crushed stone surface is shown in Figure 5.



Figure 5 – The surface area of crushed stone with bitumen as a result of the decomposition of bitumen emulsion: a) without additives; b) with ZSHO Pavlodar CHP-2; c) with ZSHO Pavlodar CHP-3

3. Results and Discussion

The average chemical composition of ash and slag waste of the surveyed CHP-2, CHP-3 of Pavlodar is shown in Table 1 [12].

Table 1 – Limits of the average content of the main components of the ash (ash and slag waste)

Component	Average content, %		Component	Average content, %	
	from - to	average		from - to	average
SiO ₂	51–60	54,5	CaO	3,0–7,3	4,3
TiO ₂	0,5–0,9	0,75	Na ₂ O	0,2–0,6	0,34
Al ₂ O ₃	16–22	19,4	K ₂ O	0,7–2,2 1	1,56
Fe ₂ O ₃	5–8	6,6	SO ₃	0,09–0,2	0,14
MnO	0,1–0,3	0,14	P ₂ O ₅	0,1–0,4	0,24
MgO	1,1–2,1	1,64	c.l.	5,8–18,8	10,6

The technological scheme of the plant for the production of cement asphalt concrete is shown in Figure 6.

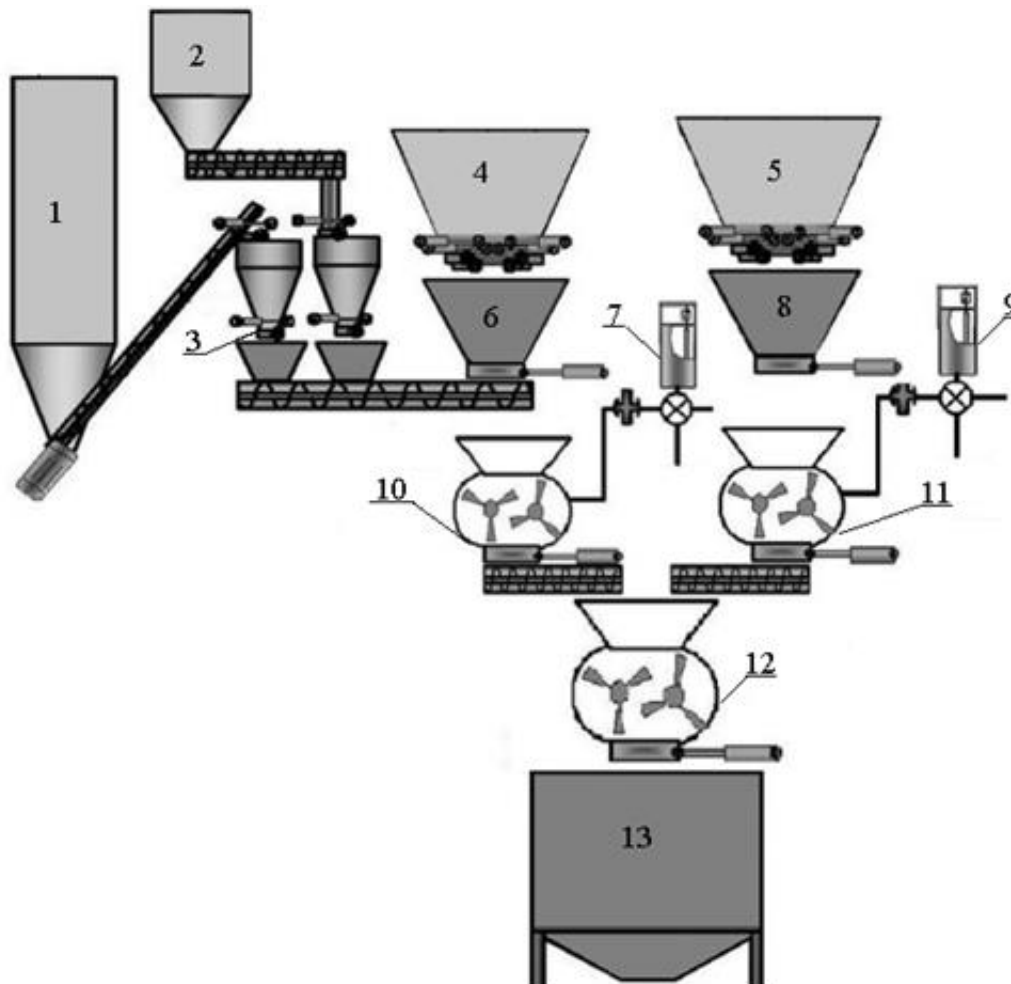


Figure 6 – Technological scheme of the plant for the production of cement asphalt concrete: 1 – cement warehouse; 2 – mineral additive warehouse; 3 – cement and additives dispenser; 4,5 – storage bins; 6 – sand dispenser; 7 – water dispenser; 8 – rubble dispenser; 9 – bitumen emulsion dispenser; 10 – mixer for cement-ash-sand mortar; 11 – mixer for black rubble; 12 – mixer for cement asphalt concrete mix; 13 – storage of cement asphalt concrete mixture

The technology of construction of structural layers of pavement made of cement asphalt concrete includes the following main stages:

Stage 1. Preparation of cement-asphalt concrete mixture at an asphalt concrete plant using stationary mixers of forced mixing.

Stage 2. Transportation of the organomineral mixture by dump trucks directly to the installation site. Taking into account the features of the resulting mixture (the presence of a hydration type of hardening binder closed with water with limited setting times), the maximum transportation time does not exceed 30 minutes at an ambient temperature of 20-30 °C and 1 hour at a temperature below 20 °C.

Stage 3. Distribution of semi-rigid composite material using an asphalt paver of any type.

Stage 4. Compaction of cement asphalt concrete mixture. The resulting material is compacted using the technology of rolled concrete.

4. Conclusions

As a result of the analysis of domestic and foreign literature, the possibility and expediency of using fine mineral materials of various natures as part of emulsion systems for their stabilization has been established, and the main criteria for mineral materials have been identified. One of the promising types of mineral raw materials for the modification of bitumen emulsions are fuel ash, however, due to the lack of experimental data, determining the effectiveness and expediency of their use is one of the most important tasks. This will expand the range of modifying additives to stabilize emulsion systems and increase the use of fuel ash.

It is advisable to consider in the direction of expanding the mineral resource base of modifying additives for the production of cement asphalt concrete, as well as analyzing the physical and mechanical characteristics and structural transformations of the structural layers of pavement made of cement asphalt concrete during operation

References

1. Innovational Construction Materials of LLP "EcostroyNII-PV" Production / K.Sh. Aryngazin, A.V. Bogomolov, A.K. Tleulessov // Defect and Diffusion Forum. — 2021. — Vol. 410. — P. 806–811. <https://doi.org/10.4028/www.scientific.net/DDF.410.806>
2. Perspektivy ispolzovaniya othodov teplovyh energocentralei AO «Aluminii Kazakhstana» / K.Sh. Aryngazin, M.B. Zhusupov, D.A. Aligozhina // Science and Technology of Kazakhstan. — 2016. — Vol. 3_4. — P. 28–34.
3. Temperature Sensitivity of Mechanical Properties of Cement Asphalt Mortar with Nanoparticles / X. Wu, X.-L. Fan, J.-F. Wang // Advances in Civil Engineering. — 2020. — Vol. 2020. — P. 1–14. <https://doi.org/10.1155/2020/3109612>
4. Asphalt Portland Cement Concrete Composite: Laboratory Evaluation / I.L. Al-Qadi, H. Goulu, R.E. Weyers // Journal of Transportation Engineering. — 1994. — Vol. 120, No. 1. — P. 94–108. [https://doi.org/10.1061/\(ASCE\)0733-947X\(1994\)120:1\(94\)](https://doi.org/10.1061/(ASCE)0733-947X(1994)120:1(94))
5. Mechanical properties of hot-mix asphalt made with recycled concrete aggregates coated with bitumen emulsion / A.R. Pasandín, I. Pérez // Construction and Building Materials. — 2014. — Vol. 55. — P. 350–358. <https://doi.org/10.1016/j.conbuildmat.2014.01.053>
6. Characterisation of Permanent Deformation Behaviour of Asphalt Mix Based on a Combined Elastic Plastic (CEP) Parameter / A.B. Roy-Chowdhury, M.F. Saleh, M. Moyers-Gonzalez // Infrastructures. — 2021. — Vol. 6, No. 12. — P. 183. <https://doi.org/10.3390/infrastructures6120183>
7. Effect of cement kiln dust on the low-temperature durability and fatigue life of hot mix asphalt / A. Modarres, H. Ramyar, P. Ayar // Cold Regions Science and Technology. — 2015. — Vol. 110. — P. 59–66. <https://doi.org/10.1016/j.coldregions.2014.11.010>
8. Sposob prigotovleniya cementno-asfaltobetonnoj smesi i ee sostav: pat. RU 2436888 / Stepashov N.E., Evtushenko S.V., Miroshnichenko S.I.; publ. 2021.
9. Modern trends in the development of the construction industry in the production of building materials / A. Aldungarova, K. Aryngazin, V. Larichkin, A. Abisheva, K. Alibekova // Technobius. — 2021. — Vol. 1, No. 3. — P. 0003. <https://doi.org/10.54355/tbus/1.3.2021.0003>

10. Evaluation of Coal Combustion Products in Hot-Mix Asphalt Mixture / Y. Gao, X. Wu, M. Hossain // Airfield and Highway Pavements 2021. — Virtual Conference: American Society of Civil Engineers, 2021. — P. 207–220. <https://doi.org/10.1061/9780784483510.020>
11. Review and Analysis of Hamburg Wheel Tracking Device Test Data / R. Farhana, H. Mustaque. — USA: Kansas State University Transportation Center, 2014. — 72 p.
12. The use of ash and slag waste CHP Pavlodar region / A.M. Kadyrbekov // Bulletin of the Innovative University of Eurasia. — 2016. — Vol. 61, No. 1. — P. 129–132.

Information about authors:

Kapar Aryngazin – Doctor of Technical Sciences, Professor, Department of Architecture and Design, Toraighyrov University, Pavlodar, Kazakhstan, kapar2021@gmail.com

Mariya Zhulasheva – Master Student, Department of Architecture and Design, Toraighyrov University, Pavlodar, Kazakhstan, mariya_98.kz@mail.ru

Assem Abisheva – PhD Student, Department of Civil Engineering, L.N. Gumilyov Eurasian National University, Nur-Sultan, Kazakhstan, abish_assem@mail.ru

Aygerim Takirova – MSc, Senior Lecturer, Department of Chemistry, Chemical Technology and Ecology, Kazakh University of Engineering and Technology, Nur-Sultan, Kazakhstan, adem_1996@mail.ru

Dina Aligozhina – MSc, Senior Lecturer, Department of Biology and Ecology, Toraighyrov University, Pavlodar, Kazakhstan, aligojina@mail.ru

Author Contributions:

Kapar Aryngazin – concept, resources, funding acquisition.

Mariya Zhulasheva – visualization, drafting.

Assem Abisheva – methodology, testing, modeling.

Aygerim Takirova – analysis, interpretation.

Dina Aligozhina – data collection, editing.

Received: 18.02.2022

Revised: 05.03.2022

Accepted: 09.03.2022

Published: 17.03.2022



Practical experience with modified bitumen and bituminous binders

Zhanar Kusbergenova¹, Aizhan Zhankina^{1,*}, Mkilima Timoth²

¹Department of Civil Engineering, L.N. Gumilyov Eurasian National University, Nur-Sultan, Kazakhstan

²Ardhi University, Plot Number 3 Block L, Observation Hill, P. O. Box 35176, Dar Es Salaam, Tanzania

*Correspondence: zhankina90@mail.ru

Abstract. To date, the issue of polymer waste recycling becomes relevant, because every year the amount of plastic and polyethylene waste increases, which leads to devastating effects on flora and fauna everywhere. One of the ways to solve this problem of polymer waste recycling is to use them to modify asphalt-concrete mixture and bitumen. Thus, two problems are solved at once: reuse of plastic, polyethylene, and other polymer wastes and improvement of asphalt concrete pavement with an increase in its service life. The paper presents a discussion of the use of modified bitumen in the construction of highways and roads, the design and technological solutions, features of the technology of modified bitumen, as well as the results of laboratory tests of modified bitumen, based on which was decided on the advisability of using. The use of the combined approach of the road pavement allows increasing the service life of the road.

Keywords: bitumen, test, safety, road pavement, mixture.

1. Introduction

1.1 Bitumen modifying additives

All over the world during the last decades, the question of finding the optimal and effective composition of bitumen that meets all the requirements for its use and further operation has been actively studied. So, in particular, some types of modifiers improve the adhesive, cohesive and other properties of bitumen, but are harmful to the environment when mixed with bitumen and further use of such bitumen for road paving [1-2]. Other modifiers meet all the requirements, but the composition of the binder in such mixtures is very expensive and, therefore, such a composition is no longer profitable in economic terms.

Every year the amount of plastic and polyethylene waste increases, which leads to destructive effects on flora and fauna everywhere. One of the ways to solve the mentioned problem of polymer waste recycling is their use in the modification of asphalt-concrete mixture and bitumen [3–7]. Thus, two problems are solved at once: reuse of plastics, polyethylene, and other polymer waste and improvement of asphalt concrete pavement with an increase in its service life. All bitumen modifying additives can be divided into several groups [8–10]:

- 1) thermoplastic polymers, they include styrene-butadiene-styrene (SBS), styrene-isoprene-styrene (SIS), styrene-ethylene/butylene-styrene (SE/BS);
- 2) Elastomers, these include rubbers and rubber-like polymers;
- 3) thermoplastics, these include: polypropylene, polyethylene, polystyrene, polyvinyl chloride, polyvinyl acetate;
- 4) thermoplastics, include epoxy, urea, polyester, and other synthetic resins.

1.2 Problems in the road sector

Bitumen is an organic binder of black or dark brown color, consisting of a mixture of high-molecular-weight hydrocarbons and their non-metallic derivatives. Bitumen is characterized by good adhesion to mineral materials, resistance to water, and acid and alkaline solutions. Bitumen reversibly converts to the viscous state when heated. Bitumen can be thinned by organic solvents and thickened by their evaporation.

Depending on their origin bitumens are divided into natural and artificial. In the construction industry are used mainly artificial petroleum bitumen is produced from the residues of oil distillation. Bitumens are divided by consistency into solid, viscous, and liquid. Bitumens are a complex mixture of high-molecular organic substances. The main chemical elements in bitumens: carbon (70-87 %), hydrogen (8-12 %), sulfur (0,5-7 %), oxygen (0,2-12 %), nitrogen (0-2 %) [1]. Most of the bitumen used in road construction is modified because the additives improve the quality of performance properties of bitumen and the result is an actual material with improved physical, mechanical and chemical properties [11]. Figure 1 shows types of pavement failures.

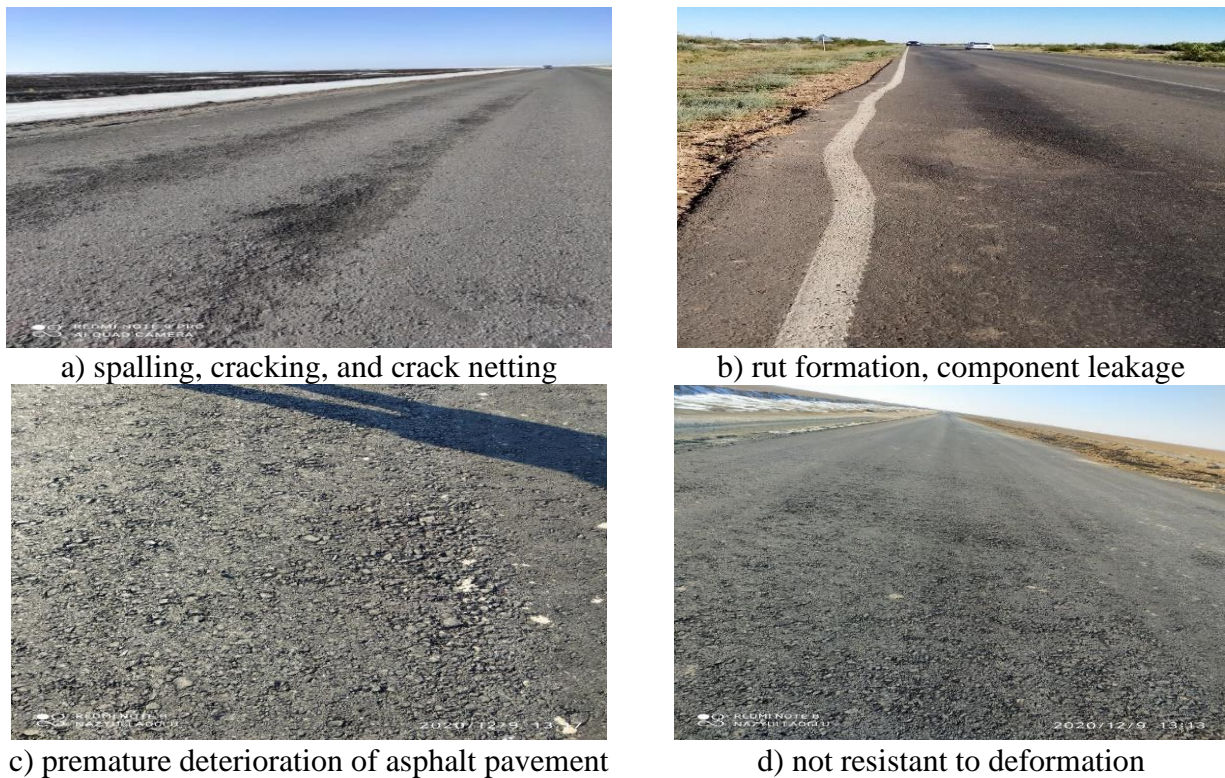


Figure 1 – Types of pavement failures [12]

2. Methods

The projected section of the highway is located in the city of Almaty. Non-injury roadway design presented in Figure 2 [13].

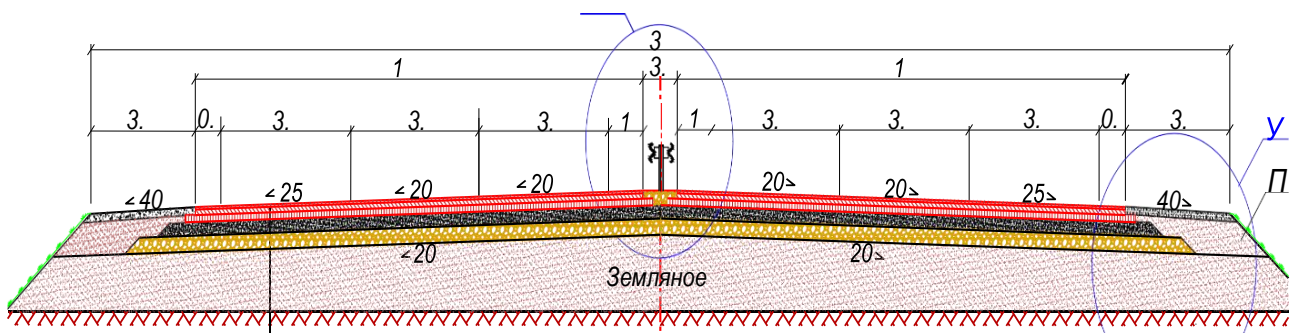


Figure 2 – Road pavement design [13]

Non-injury road pavement includes the top layer of the pavement - hot dense polymer asphalt concrete, type A, bitumen modified BMP 70/100 submark I - 5 cm; The bottom layer of the pavement - hot-laid dense asphalt concrete type A, I grade of the crushed stone mixture, grade of bitumen BND-70/100, thickness 10,0 cm; The top layer of the base - hot-laid porous asphalt concrete grade II of coarse-grained crushed stone mix, grade bitumen BND- 70/100, a thickness of 12.0 cm; The bottom layer of the basement, - crushed stone mixture C5 - 40 mm (for the foundations), a thickness of 24.0 cm; underlying layer - natural sand-gravel mixture, with a thickness of 30.0 cm. The total thickness of the pavement structure is 81 cm.

Construction of the pavement consists:

- Construction of gravel-sandy base layer and base course of crushed stone-sandy mixture
- An Additional (base) layer is made of a natural sand-gravel mixture with a thickness of 30 cm.
- The bottom layer of the base course is made of crashed stone-sandy mixture C4, with a thickness of 24 cm thickness.
- At the time of laying the mixture must have humidity close to the optimum with a deviation of not more than 10%.
- If the humidity is insufficient, moisten the mixture 20-30 minutes before the beginning of compaction.
- Distribution of the material placed in the construction layer is carried out with the help of distributors, mobile mixing plants, and motor graders.
- The layer is compacted by rollers on pneumatic tires weighing not less than 16 tons with air pressure in tires of 0.6-0.8 MPa, by trailed vibratory rollers weighing not less than Tandem vibrating rollers weighing no less than 6 tons, lattice rollers weighing no less than 15 tons, self-propelled smooth rollers weighing no less than 10 tons and combined rollers weighing more than 16 tons.
- Rolling is carried out in the longitudinal direction, with water irrigation, starting from
- The rolling is performed in the longitudinal direction, watered down from the outer edges towards the center, except for curves with curves, where except for curves and curves in which the rolling is performed from the lower edges.

Asphalt concrete pavement construction works considered:

- The top layer of the base course is made of hot porous asphalt concrete, 12 cm thick.
- The bottom pavement layer is made of hot compact coarse-grained asphalt concrete with a thickness of 10 cm.
- The top layer of the pavement is polymer asphalt concrete, 5 cm thick.

The physical and mechanical properties of the initial bitumen presented in Table 1 and of the materials are shown in Table 2.

Table 1 – Physical and mechanical properties of the initial bitumen

Indicator name	Unit of measurement	70/100	BND		ST RK		
			70/100 Spec Limits	100/130		100/130 Spec Limits	
1 – Depth of needle penetration	×0,1 mm	75	71-100	113	ST RK		
25°C					101-130	1226	
0°C					≥ 30	GOST 33136	
2 – Softening temperature in the ring and ball	°C	45.6	≥ 45	39.5	ST RK 1227 GOST 33142		
3 – Ductility at temperature:	cm	96.3	≥ 75	108	ST RK		
25°C,						≥ 90	1374
0°C						≥ 4	

						GOST 33138
4 – Flash point	°C	246	≥ 230	237	≥ 230	ST RK 1804 GOST 33141
5 – Fraas temperature brittleness	°C	-16	≤ -20	-20.5	≤ -22	ST RK 1229 GOST 33143

Table 2 – The characteristics of the materials

Specifications	Porous Asphalt		Binder Course		Wearing Course		Test Standard
	Min.	Max.	Min.	Max.	Min.	Max.	
Compaction, number of blows each end of specimen	75		75		75		TS EN 12697-30
Marshall Stability kg	600	-	750	-	900	-	TS EN 12697-34
Flow, 0.25 mm (0.01 in.)	2	5	2	4	2	4	TS EN 12697-34
Percent Air Voids %	4	6	4	6	3	5	TS EN 12697-8
Percent Voids Filled With Asphalt (VFA) %	55	75	60	75	65	75	TS EN 12697-8
Percent Voids in Mineral Aggregate (VMA) %	12	14.5	13	15	14	16	TS EN 12697-8
Filler/Bitumen	-	-	-	1.4	-	1.5	
Content of Bitumen (By weight, to 100)	3.0	5.5	3.5	6.5	4.0	7.0	TS EN 12697-1
Compressed Bituminous Mixtures Resistance Against Distortion, Indirect Tensile Strength %	80		80		80		AASHTO T 283
Wheel tracking (30.000rpm at 60 °C) max. %	-		-		8		TS EN 12697-22

3. Results and Discussion

Laboratory tests of modified bitumen according to ST RK 2534-2014 [14] are presented in Table 3 [13].

The most promising is the way to improve bitumens by polymer additives. When changing the structural and mechanical properties of used bitumens focus on the indicators of high polymers capable of maintaining the ultimate deformability at low negative temperatures, while not losing strength when heated and not softening.

Table 3 – Laboratory tests of modified bitumen

Indicator name	Unit of measurement	PMB 58-28	Test Method	35/50	50/70	70/100		100/130		130/150		Test Method
						I	II	I	II	I	II	
1 – Depth of needle penetration, at a temperature 25°C	0,1 mm	90-150	TS EN 1426	35-50	51-70	71-100		101-130		131-150		ST RK 1226 GOST 33136
2 – Softening temperature in the ring and ball	°C	≥ 45	TS EN 1427	≥ 65	≥ 62	≥ 60	≥ 58	≥ 55	≥ 52	≥ 52		ST RK 1227 GOST 33142
3 – The force ductility method	J	≥ 0,5	TS EN 13589	-	-	-	-	-	-	-	-	-
4 – The elastic recovery of modified bitumen	%	≥ 80	TS EN 13398	≥ 60	≥ 60	≥ 60	≥ 60	≥ 60	≥ 60	≥ 60		ST RK 1374 GOST 33138
5 – Flash point	°C	≥ 220	TS EN ISO 2592	≥ 240	≥ 235	≥ 230	≥ 230	≥ 230	≥ 220	220		ST RK 1804 GOST 33141

6 – Measurement of density and specific gravity	g/cm ³	1,0-1,1	TS EN 15326	-	-	-	-	-	-	-	-
7 – Dynamic Shear Rheometer, (DSR) (G*/sinδ, 1.10 kPa)	°C	≥ 58	TS EN 14770	-	-	-	-	-	-	-	-
8 – Determination of storage stability			TS EN 13399	≤ 2	≤ 2	≤ 2	ST RK 1211	≤ 2	≤ 2	≤ 2	GOST EN 13399
8.1 – Softening temperature in the ring and ball	°C	≤ 5	TS EN 1427	-	-	-	-	-	-	-	-
8.2 – Depth of needle penetration, at a temperature 25°C	0.1 mm	≤ 13	TS EN 1426	-	-	-	-	-	-	-	-

4. Conclusions

The hot polymer asphalt mixture is laid and compacted like a standard mix by conventional pavers and smooth rollers. It is recommended, if possible, that asphalt is laid across the entire width of the roadway by tracked pavers with automatic level and slope control systems. There should be no cracks or breaks in the surface of the asphalt pavement after the paver is completed. Cracks, tears, continuity defects, and other imperfections should be visible on the surface of the asphalt pavement. Detected defects can be corrected manually before the layer is compacted by adding and flattening hot mix in these areas. But the stickiness of PAS mixtures is significantly higher than conventional mixtures for dense asphalt concrete according to standards.

To obtain an even surface of the layer, it is necessary to ensure the continuity of hot polymer asphalt mixture laying is necessary to obtain a smooth surface of the layer. The recommended paving speed is at least 2-3 m/min and depends on the delivery of the asphalt mix to the pavers. For short interruptions in the delivery of the mixture, it is not recommended that it be completely discharged from the paver's hopper. The hopper should always be at least 25% full. In the case of a forced stop of the paver for 15-20 minutes, the remaining mixture from the hopper should be moved to the heated auger chamber, since hot polymer asphalt mixture mixes harder faster when cooled than standard asphalt mixtures.

References

1. Polymer modified bitumen: properties and characterisation: Woodhead Publishing in materials. — Oxford: WP, Woodhead Publ, 2011. — 404 p.
2. The Shell Bitumen Handbook / R.N. Hunter, A. Self, J. Read. — London, UK: ICE Publishin, 2015. — 761 p.
3. Effect of Waste Polyethylene and Wax-Based Additives on Bitumen Performance / L. Desidery, M. Lanotte // Polymers. — 2021. — Vol. 13, No. 21. — P. 3733. <https://doi.org/10.3390/polym13213733>
4. Performance of porous asphalt containing modified buton asphalt and plastic waste / D. S. Mabui, M. W. Tjaronge, S. A. Adisasmita and Mubassirang Pasra // International Journal of GEOMATE. — 2020. — Vol. 18, No. 65. — P. 118–123. <https://doi.org/10.21660/2020.65.67196>
5. Sustainable Practice in Pavement Engineering through Value-Added Collective Recycling of Waste Plastic and Waste Tyre Rubber / X. Xu, Z. Leng, J. Lan, W. Wang, J. Yu, Y. Bai, A. Sreeram, J. Hu // Engineering. — 2021. — Vol. 7, No. 6. — P. 857–867. <https://doi.org/10.1016/j.eng.2020.08.020>
6. Polymer modified asphalt binders / Y. Yildirim // Construction and Building Materials. — 2007. — Vol. 21, No. 1. — P. 66–72. <https://doi.org/10.1016/j.conbuildmat.2005.07.007>
7. Using Mineral Fibers to Improve Asphalt and Asphalt Mixture Behavior / L. Zhao, J. Chen, S. Wang // Traffic and Transportation Studies 2010. — Reston, VA: American Society of Civil Engineers, 2010. — P. 1352–1360. [https://doi.org/10.1061/41123\(383\)129](https://doi.org/10.1061/41123(383)129)
8. FM analysis of aging properties of UV531/SBS modified bitumen / F. Zhengang, C. Fengjie, Y. Dongdong, L. Xinjun // IOP Conference Series: Materials Science and Engineering. — 2020. — Vol. 758, No. 1. — P. 012068. <https://doi.org/10.1088/1757-899X/758/1/012068>
9. Rheological behavior of recycled polyethylene modified bitumens / E.S. Okhotnikova, I.N. Frolov, Yu.M. Ganeeva, A.A. Firsin, T.N. Yusupova // Petroleum Science and Technology. — 2019. — Vol. 37, No. 10. — P. 1136–1142. <https://doi.org/10.1080/10916466.2019.1578796>
10. Investigation of the Effect of Adhesive Additive on the Plasticity of Road Bitumen and Physical-Mechanical Properties of the Road Concrete Mix / Mukhamatdinov I. I. // Chemistry for Sustainable Development. — 2021. — No. 1. — P. 86-97. <https://doi.org/10.15372/CSD2021281>

11. Development of binder specification parameters based on characterization of damage behavior / T.P. Bahia HU, Zhai H, Zeng M, Hu Y // Journal of the Association of Asphalt Paving Technologists. — 2001. — Vol. 70. — P. 442–470.
12. Institutional Support to the National Quality Center for Road Assets [Electronic resource] / ADB. — [2020]. — Mode of access: <https://www.adb.org/projects/54092-001/main> (accessed date: 25.02.2021).
13. Working Project «Big Almaty Ring Road Construction» Survey Materials, Geological Report // «Research and Manufacturing Company Kazdorinnovaciya» LLP, Almaty. — 2019.
14. ST RK 2534-2014 Bitumen and bituminous binders. Petroleum bitumen modified, for road surface. Specifications. — 2001. — 30 p.

Information about authors:

Zhanar Kusbergenova – Master Student, Department of Civil Engineering, L.N. Gumilyov Eurasian National University, Nur-Sultan, Kazakhstan, Email: zh.kusbergenova@sapaortalygy.kz

Aizhan Zhankina – PhD Student, Department of Civil Engineering, L.N. Gumilyov Eurasian National University, Nur-Sultan, Kazakhstan, Email: zhankina90@mail.ru

Timoth Mkilima – Research Fellow, Ardhi University, Plot Number 3 Block L, Observation Hill, P. O. Box 35176, Dar Es Salaam, Tanzania, tmkilima@gmail.com

Author Contributions:

Zhanar Kusbergenova – concept, resources, interpretation, funding acquisition.

Aizhan Zhankina – data collection, testing, visualization, drafting.

Timoth Mkilima – methodology, analysis, modeling, editing.

Received: 26.02.2022

Revised: 28.02.2022

Accepted: 01.03.2022

Published: 17.03.2022



Refined mechanical and mathematical model of an elastic half-plane

Sungat Akhazhanov*, Daniyar Baltabai, Bayan Nurlanova

Faculty of Mathematics and Information Technologies, Karaganda Buketov University, Karaganda, Kazakhstan

*Correspondence: stjg@mail.ru

Abstract. Loads cause vertical movements of the foundations of all the structures. Their magnitude determines the building safe operation. A closed analytical solution to the problem of the linear elastic theory for the distribution of stresses and strains in a homogeneous isotropic elastic foundation has been presented. The article considers the calculation of the stress-strain state of an elastic half-plane by the method in displacement functions. The theory of calculating an elastic half-plane has been built. New formulas have been found that determine displacements and stresses at any points of an elastic foundation. An example of calculating an elastic half-plane under the action of a normal and tangential loads has been given.

Keywords: elastic foundation, half-plane, displacements, stresses, deformation, distribution function.

1. Introduction

Under the impact of various loads, all the structures under construction undergo greater or lesser vertical displacements (settlements), as well as horizontal shears that must be taken into account when calculating foundation bases. If the settlement values do not exceed some predetermined value, then it is considered that the long-term safe operation of the structure is ensured. In this regard, the calculation of the foundations of structures by deformations (according to the second group of limit states) is one of the most important problems of soil mechanics.

Numerous experiments have established [1] that deformations of soils under foundations develop mainly in the upper zone of the foundation, therefore, to analyze the stress-strain state of the foundations of structures, it is possible to use the calculation models based on solutions of the elastic theory [2,3].

The method of complex potentials has been used to solve a number of topical problems in the mechanics of a deformable solid body [4–6], as well as mining mechanics and soil mechanics [7,8].

Work provides a solution to the problem of stress distribution in the soil massif with a uniform displacement of the boundary section of the elastic half-plane, which was used to calculate the total settlement of the strip foundation, taking into account additional stresses arising in the soil massif due to the displacement of the loaded boundary section.

However, in practice, uneven movements are often observed that lead, for example, to the occurrence of the structure rolls. In works [9], the problems of the stress-strain state of a soil massif with linear displacement of a section of its boundary that simulates this type of the structure movement, are considered.

Andresen et al. [10] considered a means of determining the total effective bulk stress. Half-planar contacts subjected to a stressed state are considered in the following works [11-13]. Comprehensive studies of the stress-strain state of an isotropic half-plane with cracks are shown in the works [14-17].

In this article, within the framework of the model of a linearly deformable medium, the problem of the stress-strain state of an elastic half-plane is considered. The solution of the problem has been performed by the method in displacement functions.

2. Methods

To obtain the mechanical and mathematical model of an elastic half-plane, we use the method in displacement functions in solving elementary problems of the two-dimensional theory of elasticity. The method for determining the stress-strain state of an elastic half-plane makes it possible to obtain solutions to problems of the plane theory of elasticity not only for stresses, but also for displacements. Differential dependences of the stress and displacement components make it possible to obtain resolving equations for solving a specific problem.

Let's imagine an elastic foundation in the form of a half-plane and let's consider it in the Cartesian coordinate system. The stress-strain state of the elastic foundation will be determined by the calculation method in displacement functions.

To obtain a mathematical model, let's use the basic relations of the plane elastic theory [18]. Stress balance Eq. (1):

$$\begin{aligned}\frac{\partial \sigma_1}{\partial x_1} + \frac{\partial \tau_{13}}{\partial x_3} &= 0, \\ \frac{\partial \tau_{13}}{\partial x_1} + \frac{\partial \sigma_3}{\partial x_3} &= 0.\end{aligned}\quad (1)$$

Strain components (Cauchy) Eq. (2):

$$\varepsilon_1 = \frac{\partial U_1}{\partial x_1}, \quad \varepsilon_3 = \frac{\partial U_3}{\partial x_3}, \quad \gamma_{13} = \frac{\partial U_1}{\partial x_3} + \frac{\partial U_3}{\partial x_1}.\quad (2)$$

Physical relationships (Hooke law) Eq. (3):

$$\begin{aligned}\varepsilon_1 &= \frac{1}{E}(\sigma_1 - \nu \sigma_3), \quad \varepsilon_3 = \frac{1}{E}(\sigma_3 - \nu \sigma_1), \quad \gamma_{13} = \frac{\tau_{13}}{G}, \\ G &= \frac{E}{2(1+\nu)},\end{aligned}\quad (3)$$

where: σ_1, σ_3 are the components of normal stresses along the (x_1, x_3) axes; τ_{13} is a tangential stress; U_1, U_3 are the components of displacements in the direction of coordinate axes (x_1, x_3) ; $\varepsilon_1, \varepsilon_3$ are linear deformations; γ_{13} is the shear deformation; E, G, ν are the elasticity modulus, the shear modulus and the Poisson coefficient of the elastic foundation material.

Based on Eq. (2), the components of stresses Eq. (3) will take the form Eq. (4):

$$\begin{aligned}\sigma_1 &= \bar{E} \left(\frac{\partial U_1}{\partial x_1} + \nu \frac{\partial U_3}{\partial x_3} \right), \\ \sigma_3 &= \bar{E} \left(\frac{\partial U_3}{\partial x_3} + \nu \frac{\partial U_1}{\partial x_1} \right), \\ \tau_{13} &= G \left(\frac{\partial U_1}{\partial x_3} + \frac{\partial U_3}{\partial x_1} \right),\end{aligned}\quad (4)$$

where: $\bar{E} = \frac{E}{1-\nu^2}$ is the generalized elasticity modulus.

Substituting Eq. (4) into the first equation of system Eq. (1), we obtain the balance equation relative to displacements:

$$\left[\frac{\bar{E}}{G} \frac{\partial^2}{\partial x_1^2} + \frac{\partial^2}{\partial x_3^2} \right] (U_1) + \left(1 + \nu \frac{\bar{E}}{G} \right) \frac{\partial^2}{\partial x_1 \partial x_3} (U_3) = 0.$$

By expressing the components of displacements through the function of displacements F , let's determined the solution as follows Eq. (5):

$$\begin{aligned} U_3 &= \frac{\bar{E}}{G} \frac{\partial^2 F}{\partial x_1^2} + \frac{\partial^2 F}{\partial x_3^2}, \\ U_1 &= - \left(1 + \nu \frac{\bar{E}}{G} \right) \frac{\partial^2 F}{\partial x_1 \partial x_3}, \end{aligned} \tag{5}$$

where: $F(x_1, x_3)$ is the function of displacement.

Substituting stresses Eq. (4) into the second expression of system Eq. (1), we obtain:

$$\left(1 + \nu \frac{\bar{E}}{G} \right) \frac{\partial^2 U_1}{\partial x_1 \partial x_3} + \left[\frac{\partial^2}{\partial x_1^2} + \frac{\bar{E}}{G} \frac{\partial^2}{\partial x_3^2} \right] (U_3) = 0.$$

Substituting Eq. (5) into this equation, let's determine the resolving equation for F :

$$\frac{\partial^4 F}{\partial x_1^4} + \left[-2\nu + (1-\nu^2) \frac{\bar{E}}{G} \right] \frac{\partial^4 F}{\partial x_1^2 \partial x_3^2} + \frac{\partial^4 F}{\partial x_3^4} = 0.$$

Taking into consideration the \bar{E} and G values, we obtain the equation in the standard form Eq. (6):

$$\nabla^2 \nabla^2 F = \frac{\partial^4 F}{\partial x_1^4} + 2 \frac{\partial^4 F}{\partial x_1^2 \partial x_3^2} + \frac{\partial^4 F}{\partial x_3^4} = 0. \tag{6}$$

Based on Eq. (5), components of stresses Eq. (4) will be as follows Eq. (7):

$$\begin{aligned} \sigma_1 &= -\bar{E} \frac{\partial}{\partial x_3} \left(\frac{\partial^2 F}{\partial x_1^2} - \nu \frac{\partial^2 F}{\partial x_3^2} \right), \\ \sigma_3 &= \bar{E} \frac{\partial}{\partial x_3} \left(\frac{\partial^2 F}{\partial x_3^2} + (2 + \nu) \frac{\partial^2 F}{\partial x_1^2} \right), \\ \tau_{13} &= \bar{E} \frac{\partial}{\partial x_1} \left(\frac{\partial^2 F}{\partial x_1^2} - \nu \frac{\partial^2 F}{\partial x_3^2} \right). \end{aligned} \tag{7}$$

In order to solve biharmonic Eq. (6), let's represent the function of displacement in the following form [19] Eq. (8):

$$F(x_1, x_3) = \delta(x_3) \cdot W(x_1), \tag{8}$$

where: $\delta(x_3)$ is the distribution function; $W(x_1)$ is the flexure function.

Taking into consideration function of displacement Eq. (8) and the equation of transitional processes $\frac{d^2W(x_1)}{dx_1^2} = -\bar{k}^2W(x_1)$; $\frac{d^4W(x_1)}{dx_1^4} = \bar{k}^4W(x_1)$, let's find components of displacements Eq. (5) and components of stresses Eq. (7):

$$\begin{aligned}
 U_1 &= -\left(1 + \nu \frac{E}{1-\nu^2} \frac{2(1+\nu)}{E}\right) \cdot \delta'(x_3) \frac{dW(x_1)}{dx_1} = -h \left(\frac{1+\nu}{1-\nu}\right) \cdot \delta'(z_0) \frac{dW(x_1)}{dx_1}, \\
 U_3 &= \frac{E}{1-\nu^2} \frac{2(1+\nu)}{E} \cdot \frac{d^2W(x_1)}{dx_1^2} \cdot \delta(x_3) + W(x_1) \cdot \delta''(x_3) = \left[-\frac{2\bar{k}^2h^2}{1-\nu} \cdot \delta(z_0) + \delta''(z_0)\right] \cdot W(x_1), \\
 \sigma_1 &= -\bar{E} \frac{\partial}{\partial x_3} \left(\delta(x_3) \frac{d^2W(x_1)}{dx_1^2} - \nu \cdot W(x_1) \delta''(x_3) \right) = -\frac{12\bar{E}h}{12} \left[\delta'(z_0) + \frac{\nu}{\bar{k}^2h^2} \delta'''(z_0) \right] \frac{d^2W(x_1)}{dx_1^2}, \\
 \sigma_3 &= \bar{E} \frac{\partial}{\partial x_3} \left[\delta''(x_3) \cdot W(x_1) + (2+\nu) \cdot \delta(x_3) \frac{d^2W(x_1)}{dx_1^2} \right] = \\
 &= \frac{12\bar{E}h^3}{12\bar{k}^4h^4} \left[\delta'''(z_0) - (2+\nu) \cdot \bar{k}^2h^2 \delta'(z_0) \right] \frac{d^4W(x_1)}{dx_1^4}, \\
 \tau_{13} &= \bar{E} \frac{\partial}{\partial x_1} \left(\delta(x_3) \frac{d^2W(x_1)}{dx_1^2} - \nu \cdot W(x_1) \delta''(x_3) \right) = \frac{12\bar{E}h^2}{12} \left[\delta(z_0) + \frac{\nu}{\bar{k}^2h^2} \delta''(z_0) \right] \frac{d^3W(x_1)}{dx_1^3}.
 \end{aligned}$$

Based on these equations, we obtain Eq. (9) and Eq. (10):

$$\begin{aligned}
 U_1(x_1, x_3) &= -h \cdot \varphi(z_0) \frac{dW(x_1)}{dx_1}, \\
 U_3(x_1, x_3) &= f(z_0) \cdot W(x_1), \\
 \varphi(z_0) &= \frac{(1+\nu)}{(1-\nu)} \delta'(z_0), \quad f(z_0) = \delta''(z_0) - \frac{2}{(1-\nu)} k^2 \delta(z_0), \\
 z_0 &= \frac{x_3}{h}; \quad k^2 = \bar{k}^2 \cdot h^2,
 \end{aligned} \tag{9}$$

where: h is the elastic foundation thickness; z_0 is a dimensionless transversal coordinate; $\varphi(z_0), f(z_0)$ is the function of displacement distribution (U_1, U_3); \bar{k} is the strained foundation parameter.

$$\begin{aligned}
 \sigma_1 &= -\frac{\bar{E}h}{12} \cdot \psi'(z_0) \frac{d^2W(x_1)}{dx_1^2}, \\
 \tau_{13} &= \frac{\bar{E}h^2}{12} \cdot \psi(z_0) \frac{d^3W(x_1)}{dx_1^3}, \\
 \sigma_3 &= \frac{\bar{E}h^3}{12} \cdot \alpha(z_0) \frac{d^4W(x_1)}{dx_1^4}, \\
 \psi(z_0) &= 12 \left[\delta(z_0) + \frac{\nu}{k^2} \delta''(z_0) \right], \quad \alpha(z_0) = \frac{12}{k^4} \left[\delta'''(z_0) - (2+\nu) k^2 \delta'(z_0) \right],
 \end{aligned} \tag{10}$$

$$z_0 = \frac{x_3}{h}; \quad k^4 = \bar{k}^4 \cdot h^4,$$

where: $\psi'(z_0), \psi(z_0), \alpha(z_0)$ is the function of stress distribution $\sigma_1, \tau_{13}, \sigma_3$.

Substituting into resolving Eq. (6) function of displacement Eq. (8) and taking into account the equation of transitional processes, we obtain:

$$\begin{aligned} \delta(x_3) \cdot \frac{d^4 W(x_1)}{dx_1^4} + 2\delta''(x_3) \cdot \frac{d^2 W(x_1)}{dx_1^2} + \delta^{IV}(x_3) \cdot W(x_1) &= 0, \\ \left[\delta^{IV}(z_0) - 2 \cdot \bar{k}^2 h^2 \delta''(z_0) + \bar{k}^4 h^4 \delta(z_0) \right] \cdot W(x_1) &= 0, \\ \delta^{IV}(z_0) - 2 \cdot k^2 \delta''(z_0) + k^4 \delta(z_0) &= 0. \end{aligned}$$

Its general solution is written down in the following form:

$$\delta(z_0) = (C_1 + C_2 z_0) e^{-kz_0} + (C_3 + C_4 z_0) e^{kz_0} = (A_1 + A_2 z_0) chkz_0 + (A_3 + A_4 z_0) shkz_0.$$

If to use the general solution in the elastic half-plane ($z_0 \rightarrow \infty, \delta(z_0) = 0$), then this solution will take the form Eq. (11):

$$\delta(z_0) = (C_1 + C_2 z_0) e^{-kz_0}. \tag{11}$$

Thus, if the functions $W(x_1)$ and $\delta(z_0)$, are known, then the proposed method of calculation makes it possible to obtain the stress-strain state for the elastic half-plane.

3. Results

Similar problems (rigid punch, semi-infinite plane) were considered by Sadovsky for a punch and by Flaman (action of a concentrated force). These problems have the following features: it is impossible to determine the values of the reactive pressure at the corner points of the stamp; it is impossible to determine the vertical displacement under the force. These shortcomings in the considered problems are easily eliminated by applying the method in displacement functions.

Example. Let a normal $\sigma(x_1)$ and tangential $\tau(x_1)$ distributed loads act on the elastic half-plane ($z_0 = 0$). Based on Eq. (10), we write the boundary conditions in the form Eq. (12):

$$\begin{aligned} \tau_{13} = \tau: \beta_0 \frac{\bar{E}h^2}{12} \frac{d^3 W(x_1)}{dx_1^3} = \tau(x_1); \quad \psi(0) = \beta_0, \\ \sigma_3 = \sigma: \alpha_0 \frac{\bar{E}h^3}{12} \frac{d^4 W(x_1)}{dx_1^4} = \sigma(x_1); \quad \alpha(0) = \alpha_0, \end{aligned} \tag{12}$$

where: α_0, β_0 are the parameters of the normal and tangential loads.

Let's consider some private cases.

1) If the normal load $\sigma(x_1) = \sigma_0 \sin \frac{\pi x_1}{L}$ act on an elastic half-plane, then $\beta_0 = 0, \alpha_0 \neq 0$,

based on Eq. (12):

$$\alpha_0 \frac{\bar{E}h^3}{12} \frac{d^4 W(x_1)}{dx_1^4} = \sigma_0 \sin \frac{\pi x_1}{L}.$$

By integrating the equation, we obtain the flexure function Eq. (13):

$$W(x_1) = W_0 \sin \frac{\pi x_1}{L}; \quad W_0 = \frac{\sigma_0 L^4}{\alpha_0 \pi^4 E J_0}, \quad J_0 = \frac{h^3}{12}. \quad (13)$$

2) If only a tangential load $\tau(x_1) = \tau_0 \cos \frac{\pi x_1}{L}$ acts on an elastic half-plane, then $\beta_0 \neq 0$, $\alpha_0 = 0$, based on Eq. (12):

$$\beta_0 \frac{E h^2}{12} \frac{d^3 W(x_1)}{dx_1^3} = \tau_0 \cos \frac{\pi x_1}{L}.$$

By integrating we find the flexure function Eq. (14):

$$W(x_1) = -W_0 \sin \frac{\pi x_1}{L}, \quad W_0 = \frac{\tau_0}{\beta_0 \pi^3} \cdot \frac{L^3}{E J_1}, \quad J_1 = \frac{h^2}{12}. \quad (14)$$

In the general case $\beta_0 \neq 0$, $\alpha_0 \neq 0$, the, taking into consideration Eq. (10), boundary conditions Eq. (12) will be represented in the following form Eq. (15):

$$\begin{aligned} \psi(0) = \beta_0 : \quad \frac{\beta_0}{12} &= \delta(0) + \frac{\nu}{k^2} \delta''(0), \\ \alpha(0) = \alpha_0 : \quad \frac{k^4}{12} \alpha_0 &= \delta'''(0) - (2 + \nu) k^2 \delta'(0). \end{aligned} \quad (15)$$

Let's determine function Eq. (11) and the derivatives at the $(z_0 = 0)$ point Eq. (16):

$$\begin{aligned} \delta'(z_0) &= (-k C_1 + C_2 - k z_0 C_2) \cdot e^{-k z_0}, \\ \delta''(z_0) &= (-2k C_2 + k^2 C_1 + k^2 z_0 C_2) \cdot e^{-k z_0}, \\ \delta'''(z_0) &= (-k^3 C_1 + 3k^2 C_2 - k^3 z_0 C_2) \cdot e^{-k z_0}, \\ \delta(0) &= C_1, \quad \delta'(0) = -k C_1 + C_2, \\ \delta''(0) &= k^2 C_1 - 2k C_2, \quad \delta'''(0) = 3k^2 C_2 - k^3 C_1. \end{aligned} \quad (16)$$

Substituting these values into Eq. (15), we obtain the following system of equations:

$$\begin{aligned} \frac{\beta_0}{12} &= C_1(1 + \nu) - \frac{2\nu}{k} C_2, \\ \frac{k}{12} \alpha_0 &= C_1(1 + \nu) + \frac{(1 - \nu)}{k} C_2. \end{aligned}$$

From these equations there are determined the constants Eq. (17):

$$\begin{aligned} C_1 &= \frac{1}{12(1 + \nu)^2} [(1 - \nu)\beta_0 + 2k\nu\alpha_0], \\ C_2 &= \frac{k}{12(1 + \nu)} [k \cdot \alpha_0 - \beta_0]. \end{aligned} \quad (17)$$

Substituting the C_1, C_2 values into Eq. (11), we determine the solution of the $\delta(z_0)$ function Eq. (18):

$$\delta(z_0) = \left\{ \frac{1}{12(1+\nu)^2} [(1-\nu)\beta_0 + 2k\nu\alpha_0] + \frac{k}{12(1+\nu)} [k\alpha_0 - \beta_0]z_0 \right\} e^{-kz_0}. \quad (18)$$

To determine the components of displacements and stresses, we set the numerical data of the parameters. The parameters of the normal and tangential loads are $\beta_0 = 1, \alpha_0 = 1$, the length of the elastic half-plane is $L = 10$ m, the thickness of the elastic half-plane is $h = 3$ m, the elasticity modulus of the elastic half-plane is $\bar{E} = 30$ Pa.

The solutions of the problem have been obtained using the computer program MathCad. Figure 1 shows the flexure function of the elastic half-plane at $\bar{E} = 10, 20, 30$ Pa. The results of displacements, normal and shear stresses of the elastic half-plane are shown in Figures 2-4.

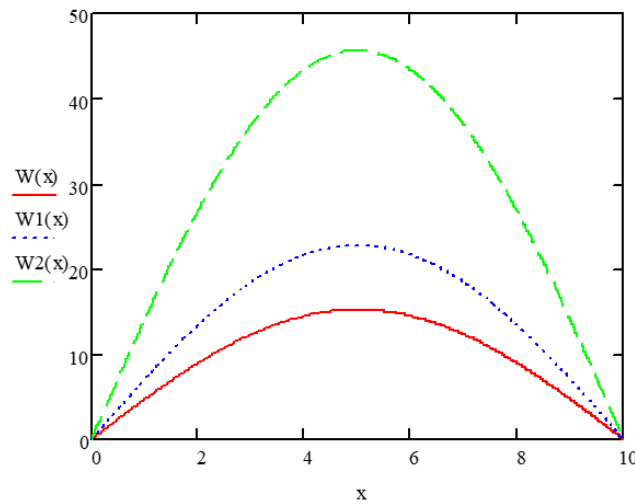


Figure 1 – The flexure function of the elastic half-plane

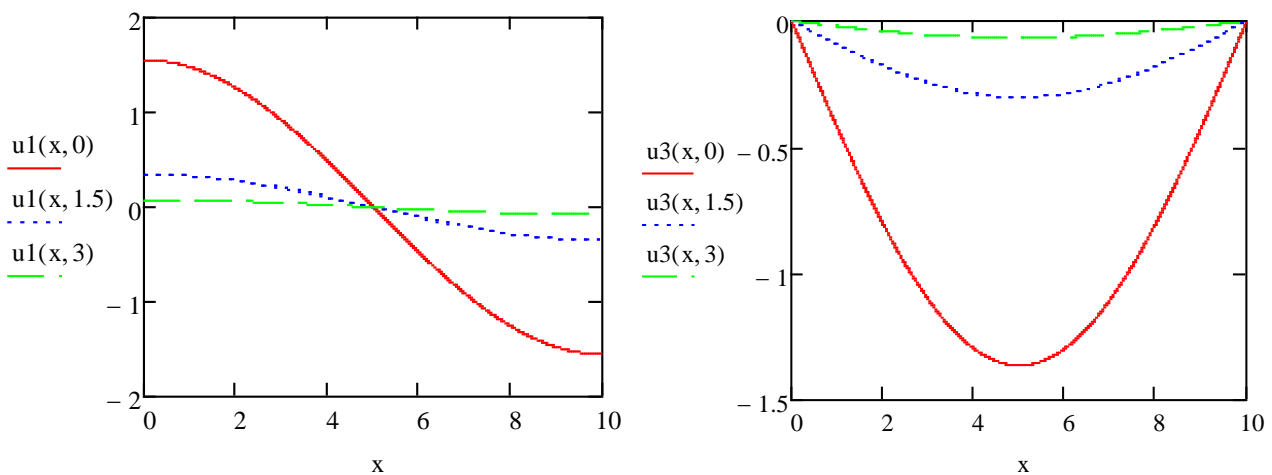


Figure 2 – The components of displacements

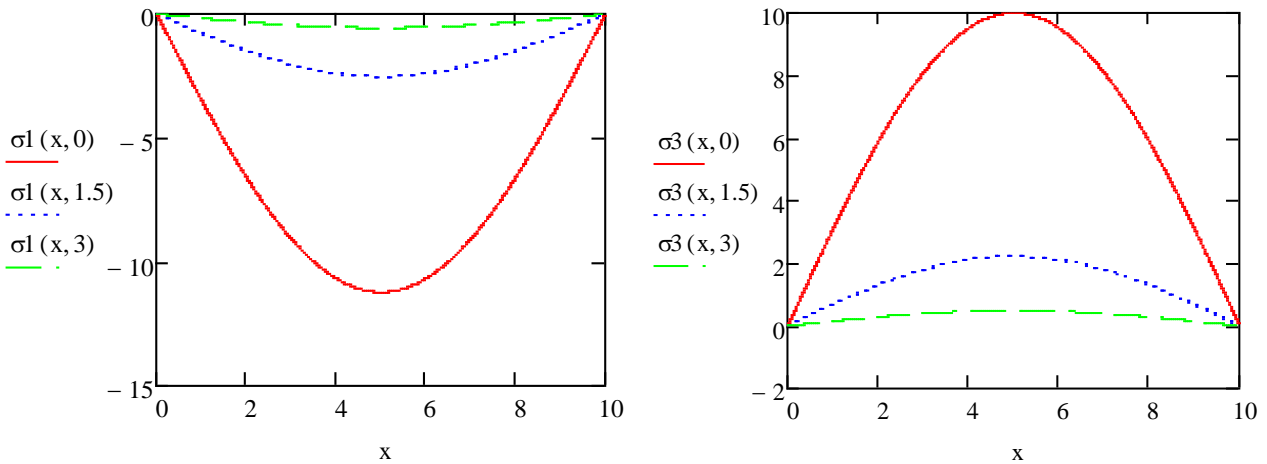


Figure 3 – The components of normal stresses

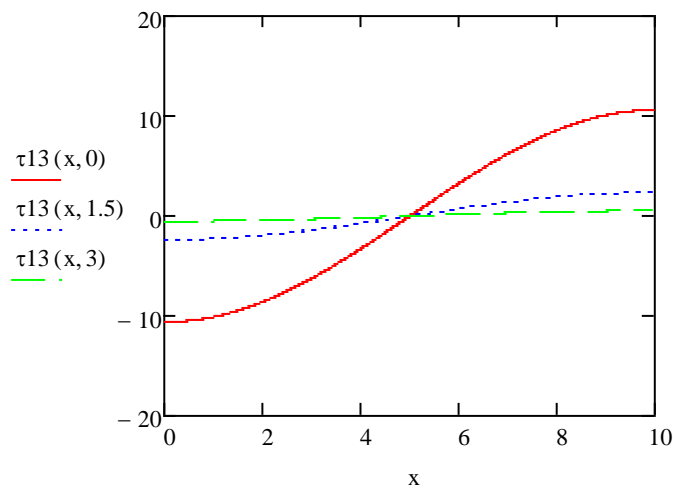


Figure 4 – A tangential stress

As can be seen from the Figures 1-4, with an increase in the thickness of the elastic foundation, the values of the components of displacements and stresses decrease. It is known that with an increase in the thickness of the elastic base, the values of the components of displacements and stresses are not taken into account.

Thus, the results obtained allow determining displacements Eq. (9) and stresses Eq. (10) of the elastic half-plane in an analytical form.

4. Conclusions

Summarizing the obtained results, we can draw the following conclusions:

1. The theory for calculating the elastic half-plane has been developed.
2. The stress and displacement components of the elastic half-plane have been obtained in a closed form.
3. The distribution functions of displacements and stresses have been found in analytical form.
4. The flexure function of the elastic half-plane has been obtained.

References

1. Mehanika gruntov, osnovaniya i fundamenti / B.I. Dalmatov. — Leningrad: Stroiizdat, 1988. — 415 p.
2. Mehanika gruntov / N.A. Tsytoich. — Moscow: Gosstroizdat, 1963. — 636 p.

3. Raschet deformacij osnovanij zdanij i sooruzhenij / S.G. Kushner. — Zaporozh'e: PLC «IPOZaporozh'e», 2008. — 496 p.
4. Complex variable methods in plane elasticity / Lu Jian-ke. — Singapore: World Scientific Pub Co Inc, 1995. — 240 p.
5. On complex variable method in finite elasticity / A. Akinola // Applied Math. — 2009. — Vol. 1. — P. 1–16.
6. Analytical Methods in Geomechanics / K.T. Chau. — Florida, USA: CRC Press, 2012. — 424 p.
7. Methods of the theory of functions of a complex variable in problems of geomechanics / A.N. Bogomolov, A.N. Ushakov. — Volgograd: Peremena, 2014. — 227 p.
8. A complex variable solutions for a deforming circular tunnel in an elastic half-plane / A. Verruijt // Numerical and Analytical Methods in Geomechanics. — 1997. — Vol. 21, No. 2. — P. 77-89. [https://doi.org/10.1002/\(SICI\)1096-9853\(199702\)21:2<77::AID-NAG857>3.0.CO;2-M](https://doi.org/10.1002/(SICI)1096-9853(199702)21:2<77::AID-NAG857>3.0.CO;2-M)
9. Stress-strain state of an elastic half-plane at a linear shift of a part of its boundary / A.N. Bogomolov, A.N. Ushakov // Vestnik MGSU. — 2017. — Vol. 12, No. 2. — P. 184-192. <https://doi.org/10.2227/1997-0935.2017.2.184-192>
10. Representation of incomplete contact problems by half-planes / H. Andresen, D. Hills, M. Moore // Eur. J. Mech. A Solids. — 2020. — Vol. 85. — P. 104138. <https://doi.org/10.1016/j.euromechsol.2020.104138>
11. Closed-form solutions for tilted three-part piecewise-quadratic half-plane contacts / H. Andresen, D.A. Hills, J. Vazquez // Int. J. Mech. Sci. — 2019. — Vol. 150. — P. 127-134. <https://doi.org/10.48550/arXiv.1902.08044>
12. Half-plane partial slip contact problems with a constant normal load subject to a shear force and differential bulk tension / M. Moore, R. Ramesh, D. Hills, et al. // J. Mech. Phys. Solids. — 2018. — Vol. 118. — P. 245-253. <https://doi.org/10.1016/j.jmps.2018.05.017>
13. Explicit equations for the half-plane sub-surface stress field under a flat rounded contact / J. Vazquez, C. Navarro, J. Dominguez // J. Strain Anal. Eng. Des. — 2014. — Vol. 49, No. 8. — P. 562-570. <https://doi.org/10.1177/0309324714545665>
14. Asymptotic analysis of stresses in an isotropic linear elastic plane or half-plane weakened by a finite number of holes / J. Kratochvil, W. Becker // Arch. Appl. Mech. — 2012. — Vol. 82. — P. 743-754. <https://doi.org/10.1007/S00419-011-0587-Z>
15. Development of a distributed dislocation dipole technique for the analysis of multiple straight, kinked and branched cracks in an elastic half plane / M.W. Hallback, N. Tofique // Int. J. Solids Struct. — 2014. — Vol. 51. — P. 2878-2892. <https://doi.org/10.1016/j.ijsolstr.2014.04.011>
16. Stress intensity factor for the interaction between a straight crack and a curved crack in plane elasticity / M.R. Aridi, N.M.A. Nik Long, Z.K. Eshkuvatov // Acta Mech. Solida Sin. — 2016. — Vol. 29. — P. 407-41. [https://doi.org/10.1016/S0894-9166\(16\)30243-9](https://doi.org/10.1016/S0894-9166(16)30243-9)
17. Evaluation of the T-stress for multiple cracks in an elastic half-plane using singular integral equation and Green's function method / Y.Z. Chen // Appl. Math. Comput. — 2014. — Vol. 228. — P. 17-30. <https://doi.org/10.1016/j.amc.2013.11.094>
18. Osnovy teorii uprugosti i plastichnosti / A.V. Alexandrov, V.D. Potapov. — Moscow: Vysshaya shkola, 1990. — 400 p.
19. Mehanika ploskih i prostranstvennyh konstrukcij / K.A. Tursunov. — Karaganda: KTU Publishing House, 2010. — 130 p.

Information about authors:

Sungat Akhazhanov – PhD, Associate Professor, Faculty of Mathematics and Information Technologies, Karaganda Buketov University, Karaganda, Kazakhstan, Email: stjg@mail.ru

Daniyar Baltabai – MSc Student, Faculty of Mathematics and Information Technologies, Karaganda Buketov University, Karaganda, Kazakhstan, Email: daniyar.baltabaj@inbox.ru

Bayan Nurlanova – Senior Lecturer, Faculty of Mathematics and Information Technologies, Karaganda Buketov University, Karaganda, Kazakhstan, Email: b.nurlanova@mail.ru

Author Contributions:

Sungat Akhazhanov – concept, methodology, resources, editing, funding acquisition.

Daniyar Baltabai – visualization, analysis, interpretation, drafting.

Bayan Nurlanova – data collection, testing, modeling.

Received: 10.03.2022

Revised: 24.03.2022

Accepted: 24.03.2022

Published: 24.03.2022



Analysis of methods for assessing the condition of surveyed facilities in Taraz City

 Alizhan Kazkeyev^{1,*},  Aleksej Aniskin²

¹Department of Civil Engineering, L.N. Gumilyov Eurasian National University, Nur-Sultan, Kazakhstan

²Department of Civil Engineering, University North, Varaždin, Croatia

*Correspondence: alizhan7sk@gmail.com

Abstract. Due to the high demand for technical inspection services for buildings and structures, new equipment designed for use in certain conditions appears on the market. On this basis, this article is devoted to the analysis of existing devices and equipment for technical inspection of buildings and structures. The analysis of equipment was carried out during the survey of 8 facilities of Novozhambyl phosphorus plant in Taraz city. In the analysis devices for non-destructive method of strength measurement were used. Based on the results obtained during the tests, the analysis was carried out. Thus, the device UKS MG4 showed the greatest deviation in the measurements when testing the reinforced concrete structures than the devices IPS MG4 and sclerometer. When controlling the reinforcement of reinforced concrete structures by electromagnetic method, the greatest accuracy of measurements showed the device Elcometer 331. The UTM-MG4 device showed a smaller error in measurements compared to a similar A1208 device. As a result of a comparative analysis of devices for determining the humidity of building materials Testo 606 showed a more reliable data, due to a different principle of operation relative to similar devices.

Keywords: technical inspection, concrete strength, non-destructive testing, comparative analysis, material strength.

1. Introduction

The development of construction in the Republic of Kazakhstan provides an increase in the number of buildings and structures erected every year in major cities of Kazakhstan [1]. In the process of their erection and further operation there is a demand for services in the field of expert activities to assess the current technical condition of buildings, inspection of buildings [2]. Such services are also required for buildings constructed in the last century. The demand for such services ensures the continuous development of the field of technical inspection of buildings and structures, which in turn leads to the appearance of new high-precision methods and devices in the market [3–6]. Some methods and devices may be relevant for specific types of structures, while others are universal [7–9]. For this reason, companies involved in technical inspection of buildings and structures are faced with the question of the best choice of one or another method and device. Also, for inspection of complex modern buildings, in view of the customer's desire to reduce stripping operations and stricter requirements for these works, it is necessary to choose the most effective methods of assessment of the inspected objects condition. The high demand for technical inspection services, as well as the inevitable obsolescence of buildings and structures make the chosen topic of this article relevant.

Based on the problems, the purpose of this article is to analyze and improve the existing methods for assessing the condition of buildings under inspection.

The object of the study are methods and instruments designed to carry out technical inspection of buildings and structures of administrative value.

In order to achieve the goal of the article, the following tasks were set and carried out:

1. Analysis of methods for assessing the technical condition of objects;
2. Analysis of non-destructive testing instruments used;
3. Analysis of survey objects in Taraz;
4. Assessment of the possibility of applying new technologies;
5. Performing theoretical research;
6. Performing experiments at construction sites in Taraz.

2. Methods

When assessing the current technical condition of the structural elements of the surveyed buildings the following operations are performed [10]: the properties of structures are determined, possible damages and defects are found, the technical condition is assessed according to categories with the possibility of their subsequent operation according to their functional purpose (as originally intended, or with changes).

To assess the current technical condition, it is necessary to compare the maximum allowable parameters of strength and deformability with the actual parameters, which are determined by the results of the survey. The calculated and normative values for the first and second groups of limiting states, respectively, are taken into account.

Figure 1 shows the principle model of the technical inspection.

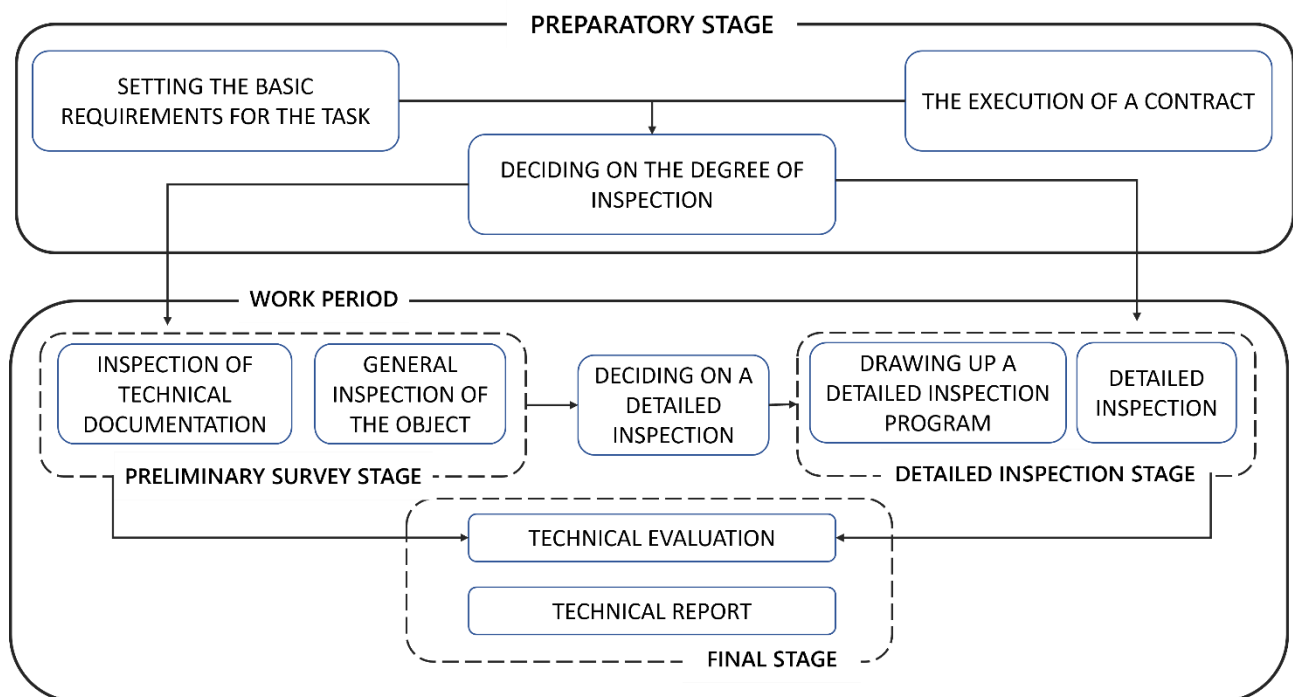


Figure 1 – Principle model of technical inspection

In the course of preparation for the survey, taking into account the agreed methodology of work performance, a preparatory stage, during which the familiarization with the objects, analysis of the available documentation, preliminary inspection, visual inspection of potentially defective areas is carried out. At the end of this stage, the need for further detailed instrumental inspection and the degree of its accuracy are established. At the next stage (detailed instrumental inspection) we make a precise methodology of work performance, calculate the number of necessary autopsies and laboratory tests and immediately the stage of survey works performance. In conclusion, on the basis of all the data obtained at the final stage, a report is prepared and recommendations for further operation are given.

The following types of structures can be subjected to survey works: wooden, steel, masonry structures, concrete and reinforced concrete.

The main criteria for assessing the current condition of reinforced concrete structures are their geometric dimensions, parameters, cracks in local areas, local cracking, nature of cracks (force, non-force), the width of their opening, the thickness of the protective layer of concrete, deformability, criteria of corrosion deterioration.

The main criteria for assessing the current condition of steel structures are: steel defects, the degree of wear of joints of steel frame elements of buildings, corrosion wear, deformability, chemical and mechanical parameters of steel, bends out of plane, displacements from the design position.

The main criteria for assessing the current state of wooden structures are: the identified defects, the presence of cracking zones, the presence of moisture zones, the presence of condensation, atmospheric effects, control of strength parameters of wood used in the manufacture of elements, as well as the quality of processing elements.

2.1 Analysis of methods for assessing the technical condition of the surveyed facilities

The main purpose of the analysis is to collect and prepare the initial materials, and then analyze the methods for assessing the technical condition of the structure of the surveyed objects for the following purposes:

- Comparative analysis of the results of the IPS MG4 [11], Sclerometer [12] and UCS MG4 [13, 14] devices for determining the strength of reinforced concrete structures.
- Comparative analysis of the results of the UCS MG4 and PULSONIC 58-E4900 [15] devices for determining the depth of cracks in reinforced concrete structures.
- Comparative analysis of the results of devices for determining the thickness of metal structures A1208 and UTM-MG4 [14].
- Comparative analysis of the results of devices for determining the humidity of building materials MG4D and Testo 606 [16].
- Advantages of the ultrasonic flaw detector A1220 MONOLITH [17] in estimating the technical condition of concrete and reinforced concrete structures.

Experimental analysis was carried out in Shop №5 of Novodzhambul phosphate plant in Taraz:

- Survey object №1 – Furnace Shop №2.
- Survey object №3 – Domestic Building №2.
- Survey object №4 – Electrode clay preparation department with storage.
- Survey object №5 – Slag dewatering bunkers of the granulation department.
- Survey object №6 – Transshipment node №6.
- Survey object №7 – Gallery №24.

2.1.1 Survey object №1

The building of the furnace shop №2 (Figure 2a) is a rectangular shape in plan with dimensions in the axes 199.25 x 65.0 m. The foundation of the building is monolithic reinforced concrete cupola type under each column separately. The main columns of the framework metal welded I-beam section. Monolithic reinforced concrete floor slabs of the building are made on the technology of permanent formwork. The bearing structures of floor slabs are metal girders of the frame. The frame girders are welded I-beams. Covering slabs are designed of precast ribbed reinforced concrete slabs. The bearing structures of the building's coverage are metal trusses. The building has a skylight. The envelope structures are single-layer wall panels and profiled sheets. Along the length of the building provides for window blocks in five rows in height. Around the building provides four fire escape stairs and two external staircases for access to the walkways on the outer perimeter of the building.

2.1.2 Survey object №2

Domestic building №2 (Figure 2b) is a rectangular shape in plan with dimensions in the axes 96.5 x 18.0 m. The building has four floors. The foundation of the building is monolithic reinforced concrete cupola type under each column separately. The walls of the basement monolithic reinforced concrete. The columns of reinforced concrete monolithic. The floor slabs are prefabricated hollow-core slabs. The bearing structures of the floor slabs are reinforced concrete girders of the frame. The floor slabs are of prefabricated hollow-core slabs. The envelope structures are single-layer wall panels. Along the length of the building is provided for window units.

2.1.3 Survey object №3

The building of the electrode clay preparation department (Figure 2c) consists of two blocks: the production part and the administrative building. The building is rectangular in plan with dimensions in the axes 18.0 x 90.5 m. The size of the industrial part in the axes is 78.0 x 18.0 m, household building 12.0 x 18.0 m. Between the blocks there is a 500 mm axial expansion joint.

The structural solution of the bearing frame of the production part is metal columns and metal trusses. Prefabricated reinforced concrete ribbed cover slabs are adopted as the cover structure.

The structural solution of the residential building is a reinforced concrete frame of precast columns, beams and slabs.

The roofing of the industrial part and the household building is flat from roll-up materials.

The walls of the industrial part of the building are constructed of expanded clay lightweight concrete wall panels of series 1.432-5 240 mm thick, the walls of the consumer building of expanded clay lightweight concrete panels according to series IIR-04. Brick sections of the outer walls are made of red brick, grade M75 on M50 mortar, 380 mm thick.

2.1.4 Survey object №4

In the granulation department (Figure 2d) there are two separately standing slag dewatering hoppers. Structures of slag dewatering bunkers are rectangular in plan with dimensions in axes 14.0x34.5 m each. The walls of bins are designed of monolithic reinforced concrete. Slabs of floor - monolithic reinforced concrete.

2.1.5 Survey object №5

Transshipment node №6 (Figure 2e) has a rectangular shape in plan with dimensions in the axes of 18x24 m. It has one floor and a basement. The functional purpose of Transshipment node №6 is to reload raw materials from gallery №24 to gallery №26.

The structural solution of the structure is a reinforced concrete frame made of columns, beams and trusses. The roof is made of precast reinforced concrete ribbed slabs on precast reinforced concrete trusses. The roof of the building is double pitch with a non-organized drain of roll materials. The foundations of the building are reinforced concrete. Enclosing structures of the gallery are profiled sheets.

2.1.6 Survey object №6

The structure (Figure 2f) is a ground overpass with enclosing structures. Gallery №24 has a total length in axes of ~60.7 m. The structure has one floor. Inside the gallery there are belt conveyors for transporting raw materials. The functional purpose of gallery № 24 is to transport raw materials from the charge department to the Transshipment node №6.

The structural solution of the structure is a reinforced concrete frame made of columns, beams and trusses. The structure of the cover is made of precast reinforced concrete ribbed slabs on precast reinforced concrete trusses. The roof of the building is double pitch with a non-organized drain of roll materials. The foundations of the building are reinforced concrete. Enclosing structures of the gallery are profiled sheets.

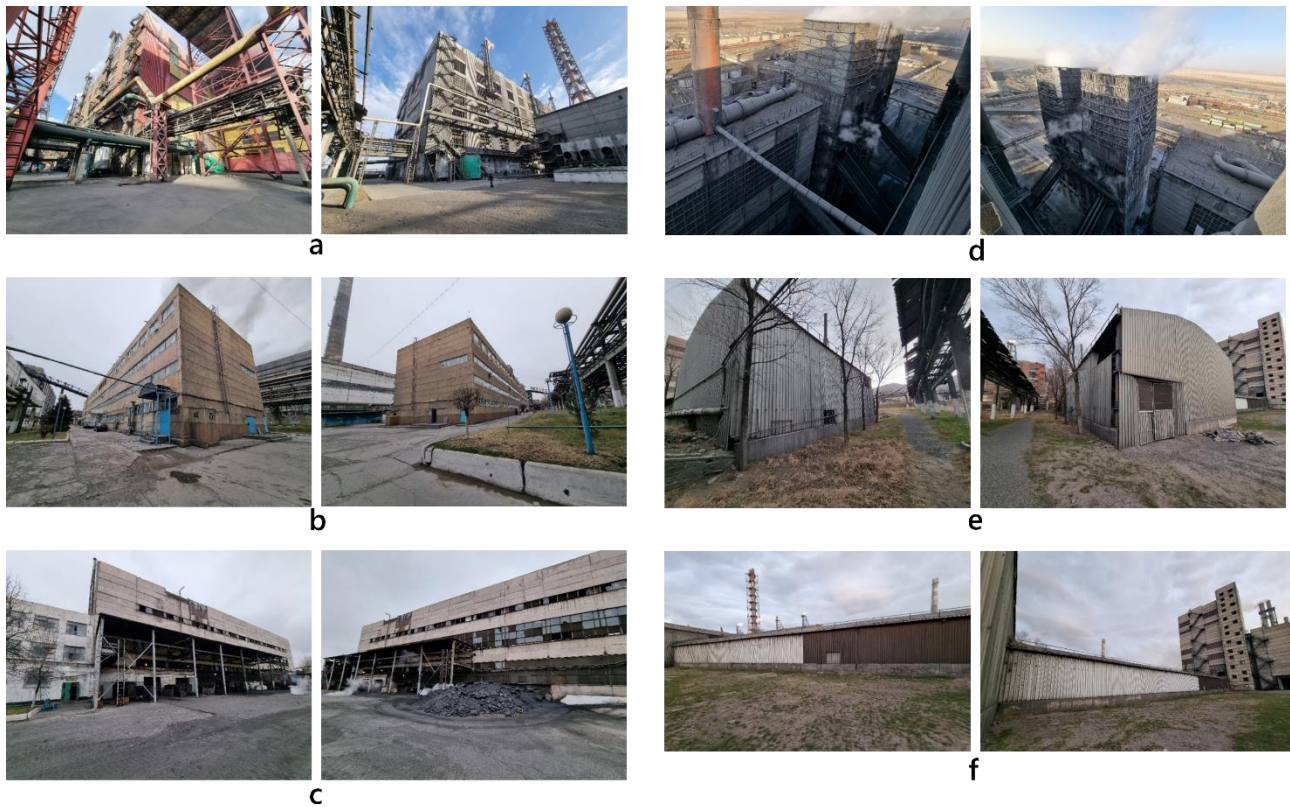


Figure 2 – General views of objects at the time of the technical survey:

a – Furnace Shop №2; b – Domestic Building №2; c – Electrode clay preparation department with storage; d – Slag dewatering bunkers of the granulation department; e – Transshipment node №6; f – Gallery №24

4. Results and Discussion

Based on the results of the technical inspection of the listed facilities, the following tables of instrument measurements were compiled.

4.1 Results of the survey of object №1

Table 1 shows the concrete strength values based on the results of nondestructive testing.

Table 1 – Concrete strength values based on the results of nondestructive testing

Structures/defects	Device results	Device results	Device results
	IPS MG4	Sclerometer	UCS MG4
Average values of foundation strength	39.6 MPa	37.4 MPa	42.2 MPa
Average strength values of columns	38.6 MPa	36.5 MPa	45.8 MPa
Average strength values of trusses	40.2 MPa	38.5 MPa	44.1 MPa
Average values of the strength of pavement slabs	37.8 MPa	36.1 MPa	39.6 MPa

According to the results, the device UCS MG4 shows more than the sclerometer, by 15-38% and IPS MG4 by 10-35%. The IPS MG4 instrument gives results greater than the sclerometer by up to 10%.

Tables 2 and 3 show the results of measurements and the results of the instruments of nondestructive testing of the protective layer of concrete of the frame and frame columns.

Table 2 – Measurement results and results of non-destructive testing of the protective layer of concrete of the frame and framework columns

Columns of a half-timbered house	IPA MG4 results, mm	Elcometer 331 results, mm
----------------------------------	---------------------	---------------------------

	48 (18)	53 (20)
	31 (20)	35 (20)

Table 3 – Measurement results and results of non-destructive testing of the protective layer of concrete of the frame and framework columns

Metal columns	Thickness gauge results A1208, mm	Results of the thickness gauge UTM-MG4, mm
<p>Columns KM1 - KM17</p>	8.06	8.02
<p>Columns KM18 – KM36</p>	6.04	6.01

According to the results of measurements of the thickness of metal columns (pipes), ultrasonic thickness gauge UTM MG4 showed an error of 0.25%, and the device A1208 with an error of 0.5%.

4.2 Results of the survey of object №2

Concrete strength of the structures was determined by non-destructive shock-pulse method using IPS-MG4 device and Digital rebound test hammer, as well as by means of UCS MG4 device. Depth of surface cracks was determined using UCS MG-4 device and PULSONIC 58-E4900 (Figure 3). Ultrasonic scanning was performed with the device MONOLITH A1220.

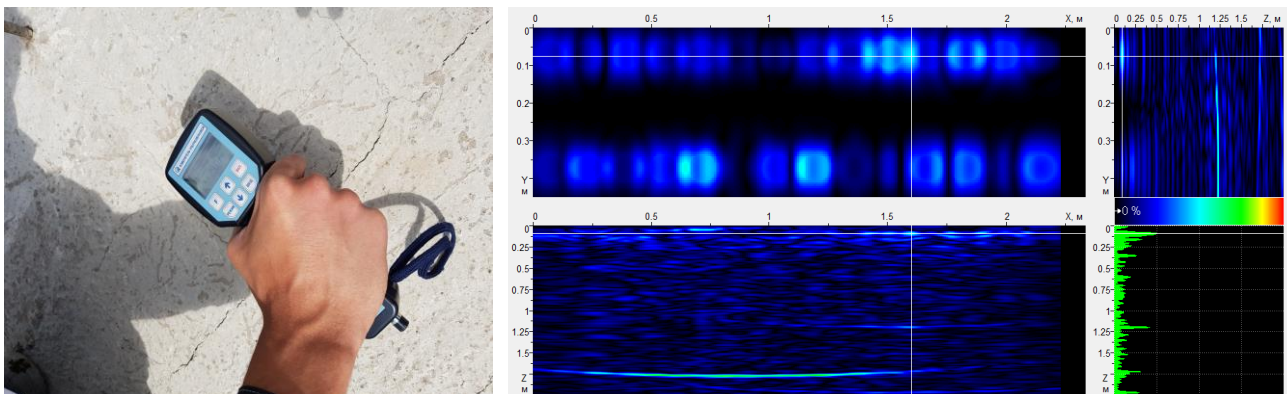


Figure 3 – Flaw detection results processed in Planevisor 4.0

The results of the flaw detector showed that closer to the surface (up to 12 centimeters) there are loose concrete.

Table 4 shows the concrete strength values based on the results of nondestructive testing.

Table 4 – Concrete strength values based on the results of nondestructive testing

Structures/defects	Device results	Device results	Device results
	IPS MG4	Sclerometer	UCS MG4
Foundation	15.6 MPa	14.3 MPa	19.4 MPa

According to the results, the device UCS MG4 shows more than the sclerometer by 35% and IPS MG4 by 25%. The result of the IPS MG4 device is greater than the sclerometer by 10%. Table 5 shows the results of the instrumental survey to determine the width and depth of cracks.

Table 5 – Results of instrumental examination to determine the width and depth of cracks

Construction	Crack No.	Width, mm	PULSONIC 58-E4900 depth	Depth results
			results, mm	UCS MG4, mm
Floor slab at +9.230, thickness 250 mm	1	0.2	281	122
	2	0.2	253	113
	3	0.2	245	120
	4	0.1	278	103
	5	0.2	238	113
	6	0.2	265	102

UCS MG4 shows such results only when a lot of pressure is applied to it, at normal pressure the device does not show anything. This is characterized by the fact that the length of the measurement base at the surface sounding of the device 120 mm.

4.3 Results of the survey of object №3

According to the results of the survey, it was found that, in general, the load-bearing capacity of the frame structures is ensured (Table 6).

Table 6 – Values of concrete strength by the results of nondestructive testing by devices IPS-MG4.01 and UCS-MG4S

Pit	Construction	Actually obtained result, MPa	Actually obtained result, MPa
1	Foundation beam	49.8	42.0
	Floor joist	43.3	40.8
	Pile 1	47.1	59.1
	Pile 2	46.5	58.7
2	Foundation beam	52.2	48.2
	Floor joist	47.6	41.3
	Pile 1	43.1	45.8
	Pile 2	47.4	48.3
3	Foundation beam	53.7	46.1
	Pile 1	48.9	58.0
	Pile 2	45.5	57.3

According to the results, the device UCS MG4 shows with an error of $\pm 25\%$ than IPS MG4.

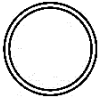
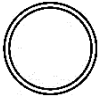
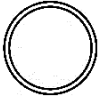
4.4 Results of the survey of object №4

Table 7 shows the values of concrete strength according to the results of nondestructive testing. Table 8 shows the results of measuring the thickness of pipes (metal columns).

Table 7 – Concrete strength values based on the results of nondestructive testing

Constructions/defects	Device results	Device results	Device results
	IPS MG4	Sclerometer	UCS MG4
Average strength values of pylons	20,5 MPa	19,5	24,2 MPa
Average strength values of precast props	36,6 MPa	35,1	29,3 MPa

Table 8 – Results of thickness measurement of pipes (metal columns)

Metal columns	Thickness gauge results	Results of the thickness gauge
	A1208, mm	UTM-MG4, mm
 Ø1020x8	8,07	8,02
 Ø820x8	8,06	8,01
 Ø426x6	6,0	6,01

According to the results of measurements of the thickness of metal columns (pipes), ultrasonic thickness gauge UTM MG4 showed an error of 0.25%, and the device A1208 with an error of 0.5%.

4.5 Results of the survey of object №5

Table 9 shows the results of moisture measurement with the MG4 and testo 606.

Table 9 – Results of moisture measurement with MG4 and Testo 606

Metal columns	Thickness gauge results	Results of the thickness gauge
	A1208, mm	UTM-MG4, mm
Rafters	14	18
Cover slab	40	35
Plastering	3	5

The difference between the results of the devices 13-22%, the reason for such results may be that the moisture meter MG4 is a surface moisture meter, and the moisture meter Testo 606 internal.

4.6 Results of the survey of object №6

Table 10 shows the values of concrete strength by the results of nondestructive testing.

Table 10 – Concrete strength values based on the results of nondestructive testing

Structures/defects	Device results	Device results	Device results
	IPS MG4	Sclerometer	UCS MG4
Average strength values of basement walls	61 MPa	55 MPa	70 MPa
Average strength values of exterior silicate brick walls	8,1 MPa	7,8 MPa	8,8 MPa

According to the results, the device UCS MG4 shows more than the sclerometer by 27% and IPS MG4 by 15%. The result of the IPS MG4 device is greater than the sclerometer by 11%.

5. Conclusions

There were comparative analyses of the results of IPS MG4, sclerometer and UKS MG4 devices to determine the strength of reinforced concrete structures. As a result, the average results of the device UCS MG4 shows deviations up to $\pm 25\%$ than the devices IPS MG4 and sclerometer. The average results of the device IPS MG4 showed 10% more than the instrument sclerometer.

Control of reinforcement of reinforced concrete structures by electromagnetic method with IPA-MG4 and Elcometer 331 devices. As a result, the IPA-MG4 device showed on average 10% less than the Elcometer 331 device.

Comparative analysis of the results of the devices for determining the thickness of metal structures A1208 and UTM-MG4. The device A1208 showed an average error of 0.5%, and the device UTM MG4 showed an average error of 0.25%.

Comparative analysis of the results of the instruments for determining the humidity of building materials MG4D and Testo 606. These devices were used at the facility number 6 and as a result of the analysis the device MG4D showed more than Testo 606 on 13-22%, as MG4D measures the moisture surface of structures, and the device Testo 606 with a penetrating method. These places dampness can be fixed by thermal imaging, which gives temperature differences in the structures.

The advantage of the ultrasonic flaw detector A1220 MONOLITH when assessing the technical condition of concrete and reinforced concrete structures is to find voids, looseness in the body of the construction.

References

1. On the commissioning of housing in the Republic of Kazakhstan / Agency for Strategic Planning and Reforms of the Republic of Kazakhstan Bureau of National Statistics. — 2021.
2. Methodology remaining lifetime determination of the building structures / Y. Otrosh, A. Kovalov, O. Semkiv, I. Rudeshko, V. Diven // MATEC Web of Conferences. — 2018. — Vol. 230. — P. 02023. <https://doi.org/10.1051/mateconf/201823002023>
3. Assessment and Inspection of the Technical Condition of Monolithic Reinforced Structures in Transportation Infrastructure Facilities / D. Topchiy, A. Bolotova // Journal of Physics: Conference Series. — 2019. — Vol. 1425, No. 1. — P. 012005. <https://doi.org/10.1088/1742-6596/1425/1/012005>
4. Use of UAVs for Technical Inspection of Buildings within the BRAIN Massive Inspection Platform / C. Serrat, A. Banaszek, A. Cellmer, V. Gibert // IOP Conference Series: Materials Science and Engineering. — 2019. — Vol. 471. — P. 022008. <https://doi.org/10.1088/1757-899X/471/2/022008>
5. Unified classification of defects detected by the technical examination / V. Klimina, A. Yurgaitis, D. Topchiy // E3S Web of Conferences. — 2019. — Vol. 110. — P. 01086. <https://doi.org/10.1051/e3sconf/201911001086>
6. Algorithm for Integrated Non-Destructive Diagnostics of Technical Condition of Structures of Buildings and Constructions Using the Thermogram Analysis / D. Karpov, A. Sinitsyn // E3S Web of Conferences. — 2020. — Vol. 161. — P. 01040. <https://doi.org/10.1051/e3sconf/202016101040>
7. Down-Sampling of Point Clouds for the Technical Diagnostics of Buildings and Structures / C. Suchocki, W. Błaszczak-Bąk // Geosciences. — 2019. — Vol. 9, No. 2. — P. 70. <https://doi.org/10.3390/geosciences9020070>
8. Technology Of Elimination Damage And Deformation In Construction Structures / A Senior Teacher, The Department Of Construction Of Buildings And Structures, Faculty Of Construction, Fergana Polytechnic Institute, Fergana City, Uzbekistan, M.U. Abdukhalimjohnovna // The American Journal of Applied sciences. — 2021. — Vol. 03, No. 05. — P. 224–228. <https://doi.org/10.37547/tajas/Volume03Issue05-35>
9. Defects search during the inspection of civil and industrial buildings and structures on the basis of laser scanning technology and information modeling approach (BIM) / A.B. Galieva, V.N. Alekhin, A.A. Antipin, S.N. Gorodilov // MATEC Web of Conferences. — 2018. — Vol. 146. — P. 01007. <https://doi.org/10.1051/mateconf/201814601007>
10. SP RK 1.04-101-2012 Survey and assessment of the technical status of buildings and constructions. — 2012.
11. Improvement of metrological measurements of bridge crossings at waterworks when studying non-destructive testing methods / M.A. Bandurin, I.P. Bandurina, I.F. Yurchenko // Journal of Physics: Conference Series. — 2021. — Vol. 1728, No. 1. — P. 012001. <https://doi.org/10.1088/1742-6596/1728/1/012001>
12. Application of a Sclerometer to the Preliminary Assessment of Concrete Quality in Structures After Fire / R. Kowalski, J. Wróblewska // Archives of Civil Engineering. — 2018. — Vol. 64, No. 4. — P. 171–186. <https://doi.org/10.2478/ace-2018-0069>
13. Research of Quality of Plasticized Concrete / A.A.M. Hasan Abbas, Y. Kupala. — Belarus: State University of Grodno, 2019. — P. 133–134.

14. Structural Analysis of Steel Membrane Roofing / A.V. Dronov // *Innovations and Technologies in Construction: Vol. 151: Lecture Notes in Civil Engineering*. — Cham: Springer International Publishing, 2021. — P. 289–295. https://doi.org/10.1007/978-3-030-72910-3_42
15. Non-destructive assessment of concrete deterioration by ultrasonic pulse velocity: A review / A. Ndagi, A.A. Umar, F. Hejazi, M.S. Jaafar // *IOP Conference Series: Earth and Environmental Science*. — 2019. — Vol. 357, No. 1. — P. 012015. <https://doi.org/10.1088/1755-1315/357/1/012015>
16. A Novel Sensor for Noninvasive Detection of In Situ Stem Water Content Based on Standing Wave Ratio / C. Gao, Y. Zhao, Y. Zhao // *Journal of Sensors*. — 2019. — Vol. 2019. — P. 1–10. <https://doi.org/10.1155/2019/3594964>
17. Detection of near-surface reinforcement in concrete components with ultrasound / S. Vonk, A. Taffe // *MATEC Web of Conferences*. — 2018. — Vol. 199. — P. 06007. <https://doi.org/10.1051/mateconf/201819906007>

Information about authors:

Alizhan Kazkeyev – PhD Student, Department of Civil Engineering, L.N. Gumilyov Eurasian National University, Nur-Sultan, Kazakhstan, alizhan7sk@gmail.com

Aleksej Aniskin – PhD, Assistant Professor, Department of Civil Engineering, University North, Varaždin, Croatia, aaniskin@unin.hr

Author Contributions:

Alizhan Kazkeyev – concept, data collection, visualization, drafting, funding acquisition.

Aleksej Aniskin – methodology, testing, modeling, interpretation, resources, analysis, editing.

Received: 28.03.2022

Revised: 30.03.2022

Accepted: 30.03.2022

Published: 30.03.2022